

# Structural Gaussian mixture vector autoregressive model with application to the asymmetric effects of monetary policy shocks

Savi Virolainen  
University of Helsinki

## Abstract

A structural version of the Gaussian mixture vector autoregressive model is introduced. The shocks are identified by combining simultaneous diagonalization of the error term covariance matrices with constraints on the time-varying B-matrix. This leads to more flexible identification conditions than in the conventional SVAR models, while some of the constraints are also testable. The empirical application considers a quarterly U.S. data covering the period from 1953Q3 to 2021Q1. Our model identifies two regimes: a stable inflation regime and an unstable inflation regime, of which the latter mainly prevails in late 1950's, 1970's, early 1980's, and during the Corona crisis. While the effects of monetary policy shocks are relatively symmetric in the unstable inflation regime, we found strong asymmetries with respect to the sign and size of the shock as well as to the initial state of the economy in the stable inflation regime. Large expansionary shocks, in particular, often drive the economy towards the unstable inflation regime and propagate high and persistent inflation. Consequently, the interest rate rises significantly, which appears to cause a strong contraction to the GDP after the initial short-term expansion. The accompanying, CRAN distributed R package `gmvarkit` provides easy-to-use tools for estimating the models and applying the introduced methods.

**Keywords:** structural nonlinear autoregression, structural mixture model, regime-switching, Gaussian mixture, mixture autoregression, monetary policy shock

---

This work was supported by the Academy of Finland under Grant 308628. The author thanks Markku Lanne, Mika Meitz, and Pentti Saikkonen who helped to improve this paper substantially. The author also thanks Henri Nyberg and Antti Ripatti for the useful comments.

Contact address: Savi Virolainen, Faculty of Social Sciences, University of Helsinki, P. O. Box 17, FI-00014 University of Helsinki, Finland; e-mail: [savi.virolainen@helsinki.fi](mailto:savi.virolainen@helsinki.fi).

The author has no conflict of interest to declare.

# 1 Introduction

Tracing out the effects of an economic shock is a major task in econometrics. A popular approach is to consider a set of key variables and utilize a structural vector autoregressive (SVAR) or error correction (SVEC) model for the purpose. They have well established theoretical grounds (see Kilian and Lütkepohl, 2017, and the references therein) and are accommodated by many of the popular statistical software. Linear SVAR and SVEC models are not, however, suitable for modelling series in which the underlying data generating dynamics are nonlinear or the shocks have asymmetric effects in different states of the economy. Models capable of capturing such features include mixture models, such as the MVAR model (Fong et al., 2010), the MPVAR model (Bentarzi and Djeddou, 2014), the GMVAR model (Kalliovirta et al., 2016), and the logit-MVAR model (Burgard et al., 2019).

Focusing on the so-called "B-model" setup, this paper introduces a structural version of the GMVAR model. In the SGMVAR model of autoregressive order  $p$ , the regime-switching dynamics are endogenously determined by the full distribution of the previous  $p$  observations. The formulation leads to attractive theoretical properties, such as ergodicity and fully known stationary distribution of  $p + 1$  consecutive observations. Moreover, it allows the researcher to associate specific characteristics to different regimes.

The effects of structural shocks are initial value dependent and also allowed to vary according to the sign and size of the shock due to the possibly resulting regime-switches. Consequently, the prevailing macroeconomic conditions, transmitted to the regime-switching probabilities through the level, variability, and temporal dependence of the past observations, are reflected to the (generalized) impulse response functions. The B-matrix of the SGMVAR model is time-varying and constructed so that it encapsulates the conditional heteroskedasticity of the reduced form error, thereby enabling us to standardize the conditional variance of the structural shock to a constant. The initial effects of a constant sized structural shock will be hence amplified according to the conditional variance of the reduced form error, further reflecting specific state of the economy.

Identification of the shocks requires that they are simultaneously orthogonalized in all regimes. We show that together with any constant standardization of the structural shock's conditional variance, this condition generally leads to a unique identification of the B-matrix up to ordering of its columns and changing all signs in a column. Thus, as long as one is willing to impose the assumption of a single (time-varying) B-matrix, the columns of the B-matrix unambiguously characterize the estimated impact effects of the economic shocks without further constraints. The identification does not, however, reveal which column of the B-matrix is related to which shock. Since the B-matrix is also subject to an estimation error, formal identification of the economic shocks requires imposing identifying constraints on its columns. The constraints are testable, as they are overidentifying.

In order to formulate the B-matrix and the identification conditions, it is convenient to utilize the well known matrix decomposition proposed by Lanne and Lütkepohl (2010) and Lanne et al. (2010) for a similar identification problem. Lanne and Lütkepohl (2010) assume that the error term covariance matrices admit this decomposition, then show that the shocks are statistically identified,

and finally test conventional zero constraints that lead to economically interpretable shocks. Lanne et al. (2010) note that the shocks are readily identified but base it on an assumption of a specific structure of the error term covariance matrices. Our approach differs from them in that we obtain locally identified structural shocks by directly investigating the properties of the B-matrix. We also provide a general set of conditions for identifying any subset of the shocks that allows to use sign constraints alone or together with zero constraints. Moreover, we (partially) relax a technical condition regarding eigenvalues related to the decomposition.

The empirical application studies asymmetries in the expected effects of monetary policy shocks in the U.S. using a quarterly series covering the period from 1954Q3 to 2021Q1. Our SGMVAR model identifies two regimes: a stable inflation regime and an unstable inflation regime, which prevails in the late 1950's, in the 1970's, in the early 1980's, and during the Corona crisis. We find the effects of monetary policy shocks relatively symmetric in the unstable inflation regime, as they rarely cause a switch to the stable inflation regime. A contractionary (expansionary) monetary policy shock appears to first increase (decrease) inflation, possibly through short-term cost-push effect, after which the inflation significantly decreases (increases) for several years. The strong contraction (expansion) in the cyclical component of GDP lasts for roughly two years and is followed by a short-term expansion (contraction) before the response decays to zero.

In the stable inflation regime, the (generalized) impulse responses are strongly asymmetric with the respect to the sign and size of the shock and to the initial state of the economy. Contractionary shocks cause a persistent contraction to the GDP but they also seem to increase inflation and drive the economy towards the unstable inflation regime. The rising prices may be explained by the cost side effects of the shock dominating the demand side effects (e.g., Barth and Ramey, 2001), but some of the movements could be also possibly attributed to an estimation error or an endogeneity problem of the identified shock. Expansionary shocks do not move prices much on average, but particularly large shocks often drive the economy towards the unstable inflation regime and propagate high and persistent inflation. As a consequence, the interest rate rises significantly, which is accompanied with a strong contraction to the GDP after the initial short term expansion.

The rest of this paper is organized as follows. Section 2 defines the reduced form GMVAR model. In Section 3, the structural GMVAR model is first introduced. Then, identification of the shocks and estimation of the model parameters are discussed. Section 4 discusses impulse response analysis and describes the generalized impulse response function (GIRF) (Koop et al., 1996). Section 5 presents the empirical application and Section 6 summarizes. Appendices provide proofs for the stated lemma and propositions, a Monte Carlo algorithm for estimating the GIRF, and details on the empirical application. Finally, we have accompanied this paper with the CRAN distributed R package `gmvar` (Virolainen, 2021a), which provides easy-to-use tools for estimating the models and applying the introduced methods.

## 2 Reduced form GMVAR model

To build theory and notation, consider first the reduced form GMVAR model introduced by Kalliovirta et al. (2016). Let  $y_t$  ( $t = 1, 2, \dots$ ) be the  $d$ -dimensional time series of interest and  $\mathcal{F}_{t-1}$  denote the

$\sigma$ -algebra generated by the random vectors  $\{y_{t-j}, j > 0\}$ . For a GMVAR model with  $M$  mixture components and autoregressive order  $p$ , we have

$$y_t = \sum_{m=1}^M s_{m,t}(\mu_{m,t} + u_{m,t}), \quad u_{m,t} \sim NID(0, \Omega_m) \quad (2.1)$$

$$\mu_{m,t} = \phi_{m,0} + \sum_{i=1}^p A_{m,i} y_{t-i}, \quad m = 1, \dots, M, \quad (2.2)$$

where  $\phi_{m,0} \in \mathbb{R}^d$  are intercept parameters,  $\Omega_m$  are positive definite covariance matrices, and for each  $m$ , the coefficient matrices  $A_{m,i}$ ,  $i = 1, \dots, p$ , are assumed to satisfy the usual stability condition

$$\det \left( I_d - \sum_{i=1}^p A_{m,i} z^i \right) \neq 0 \text{ for } |z| \leq 1, \quad m = 1, \dots, M, \quad (2.3)$$

which guarantees stationarity of the component processes. The unobservable regime variables  $s_{1,t}, \dots, s_{M,t}$  are such that at each  $t$ , exactly one of them takes the value one and the others take the value zero according to the conditional probabilities  $P(s_{m,1} = 1 | \mathcal{F}_{t-1}) \equiv \alpha_{m,t}$  that satisfy  $\sum_{m=1}^M \alpha_{m,t} = 1$ . The normally and independently distributed (NID) errors  $u_{m,t}$  are assumed independent of  $\mathcal{F}_{t-1}$ , and conditional on  $\mathcal{F}_{t-1}$ ,  $(s_{1,t}, \dots, s_{M,t})$  and  $u_{m,t}$  are independent.

The definition (2.1)-(2.2) implies that at each  $t$ , the process generates an observation from one of its mixture components, a linear VAR process, that is randomly selected according to the probabilities given by the mixing weights  $\alpha_{m,t}$ . Denoting  $\mathbf{y}_{t-1} = (y_{t-1}, \dots, y_{t-p})$ , the mixing weights are defined as (Kalliovirta et al., 2016, eq. (7))

$$\alpha_{m,t} = \frac{\alpha_m n_{dp}(\mathbf{y}_{t-1}; \mathbf{1}_p \otimes \mu_m, \Sigma_m)}{\sum_{n=1}^M \alpha_n n_{dp}(\mathbf{y}_{t-1}; \mathbf{1}_p \otimes \mu_n, \Sigma_n)}, \quad m = 1, \dots, M, \quad (2.4)$$

where  $\alpha_1, \dots, \alpha_M$  are mixing weight parameters that satisfy  $\sum_{m=1}^M \alpha_m = 1$  and  $n_{dp}(\cdot; \mathbf{1}_p \otimes \mu_m, \Sigma_m)$  is the density function of the  $dp$ -dimensional normal distribution with mean  $\mathbf{1}_p \otimes \mu_m$  and covariance matrix  $\Sigma_m$ . The symbol  $\mathbf{1}_p$  denotes a  $p$ -dimensional vector of ones,  $\otimes$  is Kronecker product,  $\mu_m = (I_d - \sum_{i=1}^p A_{m,i})^{-1} \phi_{m,0}$ , and the covariance matrix  $\Sigma_m$  is given in Lütkepohl (2005), equation (2.1.39), but using the parameters of the  $m$ th component process. That is,  $n_{dp}(\cdot; \mathbf{1}_p \otimes \mu_m, \Sigma_m)$  corresponds to the density function of the stationary distribution of the  $m$ th component process.

The mixing weights are thus weighted ratios of the component process stationary densities corresponding to the previous  $p$  observations. Consequently, the researcher can associate specific characteristics to different regimes, so in addition to the (generalized) impulse responses of the variables, responses of the mixing weights may also be of interest. The definition of the mixing weights also leads to attractive theoretical properties such as ergodicity and fully known stationary distribution of  $p$  consecutive observations (Kalliovirta et al., 2016, Theorem 1, see the proof of Theorem 1 for the stationary distribution of  $p + 1$  consecutive observations). Specifically, the stationary distribution of the process  $\mathbf{y}_t = (y_t, \dots, y_{t-p+1})$  is a mixture of  $dp$ -dimensional normal distributions that is characterized by the density

$$f(\mathbf{y}) = \sum_{m=1}^M \alpha_m n_{dp}(\mathbf{y}; \mathbf{1}_p \otimes \mu_m, \Sigma_m). \quad (2.5)$$

The knowledge of the stationary distribution is taken advantage of in the impulse response analysis in Section 4.

### 3 Structural GMVAR model

#### 3.1 The model setup

Consider the GMVAR model defined in (2.1)-(2.2). We focus on the "B-model" setup and write the structural GMVAR model as

$$y_t = \sum_{m=1}^M s_{m,t} \left( \phi_{m,0} + \sum_{i=1}^p A_{m,i} y_{t-i} \right) + B_t e_t, \quad (3.1)$$

and

$$u_t \equiv B_t e_t = \begin{cases} u_{1,t} \sim N(0, \Omega_1) & \text{if } s_{1,t} = 1 & \text{(with probability } \alpha_{1,t}) \\ u_{2,t} \sim N(0, \Omega_2) & \text{if } s_{2,t} = 1 & \text{(with probability } \alpha_{2,t}) \\ \vdots & & \\ u_{M,t} \sim N(0, \Omega_M) & \text{if } s_{1,M} = 1 & \text{(with probability } \alpha_{M,t}) \end{cases} \quad (3.2)$$

where the probabilities are expressed conditionally on  $\mathcal{F}_{t-1}$  and  $e_t$  is an orthogonal structural error. Unlike in the conventional SVAR analysis, the invertible ( $d \times d$ ) "B-matrix"  $B_t$ , which governs the contemporaneous relations of the shocks, is time-varying and a function of  $y_{t-1}, \dots, y_{t-p}$ . This enables to amplify a constant sized structural shock according to the conditional variance of the reduced form error, which varies according to the mixing weights. Appropriate modelling of conditional heteroskedasticity in the B-matrix is of interest, because the (generalized) impulse responses may be asymmetric with respect to the size of the shock.

We have  $\Omega_{u,t} \equiv \text{Cov}(u_t | \mathcal{F}_{t-1}) = \sum_{m=1}^M \alpha_{m,t} \Omega_m$ , while the conditional covariance matrix of the structural errors  $e_t = B_t^{-1} u_t$  (which have a mixture normal distribution and are not IID but are martingale differences and therefore uncorrelated) is obtained as

$$\text{Cov}(e_t | \mathcal{F}_{t-1}) = \sum_{m=1}^M \alpha_{m,t} B_t^{-1} \Omega_m B_t'^{-1}. \quad (3.3)$$

The B-matrix  $B_t$  should thus be chosen so that the structural shocks are orthogonal regardless of which regime they come from. It turns out that any such B-matrix has (linearly independent) eigenvectors of the matrix  $\Omega_m \Omega_1^{-1}$  as its columns. Moreover, the B-matrix is unique up to scalar multiples and ordering of its columns if for all  $i \neq j \in \{1, \dots, d\}$ , there exists an  $m \in \{2, \dots, M\}$  such that  $\lambda_{mi} \neq \lambda_{mj}$ , where  $\lambda_{mi}$  are the eigenvalues of  $\Omega_m \Omega_1^{-1}$ . These results are formalized in the following assumption and lemma.

**Assumption 1.** Consider  $M$  positive definite ( $d \times d$ ) covariance matrices  $\Omega_m$ ,  $m = 1, \dots, M$ , and denote the strictly positive eigenvalues of the matrices  $\Omega_m \Omega_1^{-1}$  as  $\lambda_{mi}$ ,  $i = 1, \dots, d$ ,  $m = 2, \dots, M$ . Suppose that for all  $i \neq j \in \{1, \dots, d\}$ , there exists an  $m \in \{2, \dots, M\}$  such that  $\lambda_{mi} \neq \lambda_{mj}$ .

**Lemma 1.** Consider  $M$  positive definite  $(d \times d)$  covariance matrices  $\Omega_m$ ,  $m = 1, \dots, M$ , and an invertible  $(d \times d)$  matrix  $B_t$  such that  $B_t^{-1}\Omega_m B_t'^{-1}$  are diagonal matrices with strictly positive diagonal elements. Then,  $B_t$  has eigenvectors of  $\Omega_m \Omega_1^{-1}$  as its columns. Moreover,  $B_t$  is unique up to scalar multiples and ordering of its columns if Assumption 1 holds.

By Lemma 1, any invertible B-matrix that simultaneously diagonalizes the covariance matrices has linearly independent eigenvectors of  $\Omega_m \Omega_1^{-1}$  as its columns. If  $M > 2$ , the matrices  $\Omega_m \Omega_1^{-1}$ ,  $m = 2, \dots, M$ , thus need to share the common eigenvectors in  $B_t$ , which restricts the parameter space for the covariance matrices. In this case, the existence of such B-matrix can be tested with a likelihood ratio test, for example.

Under Assumption 1, the columns of  $B_t$  are unique up to scalar multiples and ordering, implying that the shocks are identified up to sign, size and ordering of shocks. Normalizing the conditional covariance matrix of the structural error to a constant diagonal matrix then identifies the B-matrix up to sign and ordering of the shocks. This is formalized in the following proposition.

**Proposition 1.** Consider  $M$  positive definite  $(d \times d)$  covariance matrices,  $\Omega_m$ ,  $m = 1, \dots, M$ , and an invertible  $(d \times d)$  matrix  $B_t$  such that  $B_t^{-1}\Omega_m B_t'^{-1}$  are diagonal matrices with strictly positive diagonal elements. Suppose that Assumption 1 holds. Then, if the conditional covariance matrix of the structural error,  $\text{Cov}(e_t | \mathcal{F}_{t-1}) = \sum_{m=1}^M \alpha_{m,t} B_t^{-1} \Omega_m B_t'^{-1}$ , is normalized to a constant diagonal matrix with strictly positive diagonal entries, the B-matrix  $B_t$  is unique up to ordering of its columns and changing all signs in a column.

That is, by fixing an ordering and signs for the columns of the B-matrix, the solution to the diagonalization problem is unique for any given (constant) normalization of the structural error's conditional covariance matrix. The normalization is not only useful but also necessary if one does not wish to incorporate structural shocks whose conditional variance depends on the past movements of the endogenous variables. In our model, the time-varying B-matrix captures the conditional variance of the reduced form error, and thereby governs the contemporaneous relationships of the shocks according to the prevailing macroeconomic conditions.

After deciding upon the normalization of the structural error's covariance matrix, say an identity matrix, we need to find the related B-matrix. To that end, it is convenient to utilize the following matrix decomposition for the error term covariance matrices, which was also employed by Lanne and Lütkepohl (2010) and Lanne et al. (2010). We decompose the error term covariance matrices as

$$\Omega_1 = WW' \quad \text{and} \quad \Omega_m = W\Lambda_m W', \quad m = 2, \dots, M, \quad (3.4)$$

where the diagonal of  $\Lambda_m = \text{diag}(\lambda_{m1}, \dots, \lambda_{md})$ ,  $\lambda_{mi} > 0$  ( $i = 1, \dots, d$ ), contains the eigenvalues of the matrix  $\Omega_m \Omega_1^{-1}$  and the columns of the nonsingular  $W$  are the related eigenvectors (that are the same for all  $m$  by construction). When  $M = 2$ , the decomposition (3.4) always exists (Muirhead, 1982, Theorem A9.9), but for  $M \geq 3$  its existence requires that the matrices  $\Omega_m \Omega_1^{-1}$  share the common eigenvectors in  $W$ . This is, however, testable and relates to our earlier discussion on the existence of a B-matrix that simultaneously diagonalizes the error term covariance matrices.

Because  $W$  contains linearly independent eigenvectors of  $\Omega_m \Omega_1^{-1}$  as its columns, any scalar multiples of  $W$ 's columns comprise an appropriate B-matrix. But only specific scalar multiples com-

prise the locally unique B-matrix associated with a given normalization of structural error's conditional covariance matrix. Direct calculation shows that a B-matrix that amplifies a constant sized structural shock according to the conditional variance of the reduced form error is obtained as

$$B_t = W(\alpha_{1,t}I_d + \sum_{m=2}^M \alpha_{m,t}\Lambda_m)^{1/2}, \quad (3.5)$$

where  $B_t B_t' = \Omega_{u,t}$ . Since  $B_t^{-1}\Omega_m B_t'^{-1} = \Lambda_m \left(\sum_{n=1}^M \alpha_{n,t}\Lambda_n\right)^{-1}$  where  $\Lambda_1 \equiv I_d$ , the B-matrix (3.5) simultaneously diagonalizes  $\Omega_1, \dots, \Omega_M$ , and  $\Omega_{u,t}$  for each  $t$  so that the structural error's conditional covariance is normalized to an identity matrix:

$$\text{Cov}(e_t | \mathcal{F}_{t-1}) = \sum_{m=1}^M \alpha_{m,t}\Lambda_m \left(\sum_{n=1}^M \alpha_{n,t}\Lambda_n\right)^{-1} = I_d. \quad (3.6)$$

Our specification of the B-matrix differs from Lanne et al. (2010) who assume that the instantaneous effects of the shocks are time-invariant (and specify  $B_t = W$ ) but it extends the one in Lanne and Lütkepohl (2010) to accommodate time-varying mixing weights.

The SGMVAR model assumes a single B-matrix that varies continuously in time according to the conditional variance of the reduced form error, which in turn varies according to the mixing weights. We established that under Assumption 1 and a normalization of the structural error's conditional variance, the B-matrix is unique up to ordering of its columns and switching all signs in a column. Hence, as long as one is willing to impose the assumption of a single (time-varying) B-matrix, the columns of the B-matrix unambiguously characterize the estimated impact effects of the economic shocks, but they do not reveal which column is related to which shock.<sup>1</sup> Since the impact effects are also subject to an estimation error, additional constraints are required for formal identification of the structural shocks.

## 3.2 Identification of the shocks

Even if all pairs of  $\lambda_{mi}$  are distinct for some  $m$ , unique identification of  $B_t$  requires deciding upon the ordering of the eigenvalues  $\lambda_{mi}$  in the diagonals of  $\Lambda_m$ , which fixes also an ordering for the columns of  $W$ . While statistical identification of the model is achieved with any arbitrary ordering the eigenvalues, it does reveal which column is related to which economic shock, and thereby additional constraints are required for economic interpretation of the shocks. In particular, a structural shock relates to an economic shock through the specific constraints in the corresponding column of  $W$  (or equally of the B-matrix) that only the shock of interest satisfies. If such constraints are readily satisfied in the (unrestricted) estimate of  $W$ , the identification amounts to labelling the structural shocks by the appropriate economic shocks, as long as the constraints are strong

<sup>1</sup> In an alternative specification of the structural model, there would be a separate B-matrix for each of the regimes. While our B-matrix allows the magnitude of a constant sized shock to vary according to the mixing weights, it does not allow variation in the impact effects relative to the other variables. That is, our model imposes structure already in the model equations (3.1) and (3.2).

enough to pin down a unique ordering for the columns of  $W$  (this argument will be formalized in Proposition 2 below).<sup>2</sup>

If the unrestricted estimate of  $W$  is such that the researcher cannot associate the economic shocks to it, the appropriate constraints can be placed for their identification. Besides a single sign constraint in each column of  $W$ , zero and sign constraints on  $W$  are overidentifying and therefore testable. Lanne and Lütkepohl (2010) and Lanne et al. (2010) take advantage of this observation and test for conventional zero constraints in their B-matrices. We show that in the SGMVAR model, globally unique identification of the structural shocks can be achieved with more flexible conditions than in the conventional SVAR models. Furthermore, as in practice one is often interested in identifying only some specific shock or shocks, it makes sense to consider only partial identification of the B-matrix as well. Specifically, we say that the  $j$ th structural shock is uniquely identified if the  $j$ th column of the B-matrix (3.5) is unique for given mixing weights  $\alpha_{1,t}, \dots, \alpha_{M,t}$ . This requires that the  $j$ th columns of  $W$  and  $\Lambda_m, m = 2, \dots, M$ , are unique. The following proposition gives sufficient conditions for global identification of the last  $d_1$  shocks when the related pairs of  $\lambda_{mi}$  are distinct for some  $m$ .

**Proposition 2.** *Suppose  $\Omega_1 = WW'$  and  $\Omega_m = W\Lambda_mW'$ ,  $m = 2, \dots, M$ , where  $\Lambda_m = \text{diag}(\lambda_{m1}, \dots, \lambda_{md})$ ,  $\lambda_{mi} > 0$  ( $i = 1, \dots, d$ ), contains the eigenvalues of  $\Omega_m\Omega_1^{-1}$  in the diagonal and the columns of the nonsingular  $W$  are the related eigenvectors. Then, the last  $d_1$  structural shocks are uniquely identified if*

- (1) for all  $j > d - d_1$  and  $i \neq j$  there exists an  $m \in \{2, \dots, M\}$  such that  $\lambda_{mi} \neq \lambda_{mj}$ ,
- (2) the columns of  $W$  are constrained in a way that for all  $i \neq j > d - d_1$ , the  $i$ th column cannot satisfy the constraints of the  $j$ th column as is nor after changing all signs in the  $i$ th column, and
- (3) there is at least one (strict) sign constraint in each of the last  $d_1$  columns of  $W$ .

Condition (3) of Proposition 2 fixes the signs in the last  $d_1$  columns of  $W$  and therefore the signs of the instantaneous effects of the corresponding shocks. Changing the signs of the columns is effectively the same as changing the signs of the corresponding shocks, so condition (3) is not restrictive, however (as the structural shock has a distribution that is symmetric about zero). The assumption that the identified shocks are the last  $d_1$  shocks is neither restrictive as one may always reorder the structural shocks accordingly.

For example, if  $d = 3$ ,  $\lambda_{m1} \neq \lambda_{m3}$  for some  $m$ , and  $\lambda_{m2} \neq \lambda_{m3}$  for some  $m$ , the third structural shock can be identified with the following constraints:

$$B_t = \begin{bmatrix} * & * & * \\ + & + & - \\ + & + & + \end{bmatrix} \text{ or } \begin{bmatrix} - & * & + \\ - & + & - \\ * & + & + \end{bmatrix} \text{ or } \begin{bmatrix} + & 0 & - \\ * & * & * \\ + & * & + \end{bmatrix} \quad (3.7)$$

<sup>2</sup> For a more thorough discussion on economic shocks and their identification, see Ramey (2016) and Uhlig (2017), for example.

and so on, where " \* " signifies that the element is not constrained, " + " denotes a strict positive and " - " a strict negative sign constraint, and " 0 " means that the element is constrained to zero. Because imposing sign or zero constraints on  $W$  equals to placing them on  $B_t$ , they may be justified economically. Furthermore, besides a single sign constraint in each column, the constraints are overidentifying and can thus be also validated statistically. Sign constraints, however, do not reduce the dimension of the parameter space, making some of the measures such as the conventional likelihood ratio test and information criteria unsuitable for testing them. Quantile residual diagnostics (see Kalliovirta and Saikkonen, 2010), on the other hand, can be used to evaluate how well the restricted model is able to explain the statistical properties of the data compared to the unrestricted alternative.

When  $d_1 < d$  in Proposition 2, only partial identification of the B-matrix might be a concern when testing for the constraints in condition (2), as the problem of applying a test for an unidentified model is non-standard. Full statistical identification is, however, achieved by fixing an ordering for the eigenvalues  $\lambda_{mi}$  corresponding to the columns of  $W$  that are not fully identified by constraining  $W$ , as long as Assumption 1 holds. That is, as long as for all  $i, l = 1, \dots, d$  such that  $i \neq l$  there exists an  $m \in \{2, \dots, M\}$  such that  $\lambda_{mi} \neq \lambda_{ml}$ . If some of the eigenvalues are equal for all  $m$  (including the ones with  $i, l \leq d - d_1$ ), the model is not fully identified and the testing problem is non-standard despite of a fixed ordering of the eigenvalues and columns of  $W$  (testing under no identification is briefly discussed below, after Proposition 3).

Shocks that do not satisfy condition (1) of Proposition 2 can still be identified, but it requires stronger conditions. The following proposition provides sufficient criteria for global identification of the last  $d_1$  shocks when exactly one of the eigenvalues  $\lambda_{mi}$  with  $i \neq j > d - d_1$  is identical to  $\lambda_{mj}$  for all  $m$ . For simplicity, we assume that only another one of the shocks with identical eigenvalues is to be identified.

**Proposition 3.** *Let  $d_1 < d$ . Consider the matrix decomposition of Proposition 2 and further suppose that for  $j = d - d_1 + 1$  and some  $i \leq d - d_1$  we have  $\lambda_{mi} = \lambda_{mj}$  for all  $m$ , but for all  $l \notin \{i, j\}$ ,  $\lambda_{ml} \neq \lambda_{mj}$  for some  $m$ . Then, the last  $d_1$  structural shocks are uniquely identified if conditions (1)-(3) of Proposition 2 are otherwise satisfied, and in addition*

- (4) *the column  $i \leq d - d_1$  of  $W$  such that  $\lambda_{mi} = \lambda_{mj}$  for all  $m$  has at least one (strict) sign constraint and the  $j$ th column has a zero constraint where the  $i$ th column has the (strict) sign constraint.*

Note that the assumption  $j = d - d_1 + 1$  is made without loss of generality because the structural shocks can always be reordered accordingly by also reordering the columns of  $W$  (including the constraints) and the eigenvalues  $\lambda_{mi}$  correspondingly.<sup>3</sup>

To exemplify, if  $d = 4$ ,  $\lambda_{m1} \neq \lambda_{m4}$  for some  $m$ ,  $\lambda_{m2} \neq \lambda_{m4}$  for some  $m$ , and  $\lambda_{m3} = \lambda_{m4}$  for all

<sup>3</sup> While the assumptions in Propositions 2 and 3 regarding the ordering of the shocks are not restrictive, they can also be relaxed to allow for any ordering and are made here for simplicity only.

$m$ , the following constraints lead to global identification of last shock:

$$B_t = \begin{bmatrix} * & * & * & * \\ * & * & + & 0 \\ + & + & * & - \\ + & + & * & + \end{bmatrix} \text{ or } \begin{bmatrix} * & * & - & 0 \\ * & * & * & * \\ + & - & * & + \\ - & + & * & + \end{bmatrix} \text{ or } \begin{bmatrix} + & - & - & 0 \\ * & * & * & * \\ * & * & * & * \\ * & * & * & + \end{bmatrix} \quad (3.8)$$

and so on. As is demonstrated above, the structural shocks can often be identified with more flexible constraints than in conventional SVAR models even when some of the eigenvalues are identical for all the error term covariance matrices.

Under conditions (1) and (3) of Proposition 2, the additional constraints on  $W$  were stated testable because they are overidentifying and statistical identification of the model can always be achieved by fixing the order of the eigenvalues  $\lambda_{mi}$ , as long as none of the pairs of  $\lambda_{mi}$ ,  $i = 1, \dots, d$ , is identical for all  $m = 2, \dots, M$ . In the setup of Proposition 3, however, when  $\lambda_{mi} = \lambda_{mj}$  for all  $m$  and some  $i \neq j$ , the model is not generally identified even when one fixes a unique ordering for the eigenvalues and columns of  $W$ . Also, even if condition (4) of Proposition 3 is satisfied, only partial identification of the B-matrix is obtained since nothing guarantees unique identification of the  $i$ th column of  $W$ , which would require stronger conditions. Consequently, the model is not identified under the null nor the alternative hypothesis when testing for the constraints in conditions (2) and (4), making the testing problem non-standard and the conventional asymptotic distributions of the likelihood ratio and Wald test statistics unreliable. The same applies when one tests the equality of the eigenvalues in order to assess the validity of condition (1) of Proposition 2, as the model is not identified under null.

Related testing problems under no identification have attained some attention in the recent literature. Lütkepohl et al. (2021) developed an asymptotic Wald type test for testing equality of the  $\lambda_{mi}$  parameters in the context of a linear SVAR model incorporating two volatility regimes with a known change point and (reduced form) shocks arriving from a class of elliptical distributions. Meitz and Saikkonen (2021), on the other hand, studied the asymptotic properties of a likelihood ratio test statistic when testing for the number of regimes in mixture models with Gaussian conditional densities. One of the studied models is the GMAR model (Kalliovirta et al., 2015), which is the univariate counterpart of the GMVAR model (Kalliovirta et al., 2016). Such formal analysis of the test statistics under no identification is, however, a major task and beyond the scope of this paper. We therefore rely on approximate standard errors (which are asymptotically valid only if the model is statistically identified) as a pragmatic tool for assessing informally whether inequality of the eigenvalues seems plausible. If appropriate, inequality of the  $\lambda_{mi}$  is then simply assumed without formal justification.<sup>4</sup>

If more than two eigenvalues are identical for all  $m = 2, \dots, M$  but they are not all identical, it may still be possible to find more flexible conditions for identification of the shocks than in the

<sup>4</sup> An alternative strategy would be to compare the values of information criteria between the unrestricted model and a model that has some of the  $\lambda_{mi}$  constrained equal to each other in all  $m$ . But maximizing the log-likelihood function in order to obtain the values of the information criteria can be challenging in practice, because the maximum likelihood estimator does not identify under the constraint that some of the  $\lambda_{mi}$  are equal in all  $m = 2, \dots, M$  (unless also the appropriate zero constraints have been imposed). For this reason, we prefer the standard errors over the information criteria.

conventional SVAR models. Specifically, the idea utilized in the proof of Proposition 3 (presented in Appendix A) can be applied to larger numbers of identical eigenvalues. If all the eigenvalues are identical for all covariance matrices, then  $\Omega_m = \lambda_{m1}\Omega_1$  and the identification condition is the same as for the conventional SVAR model (which is given, for example, in Lütkepohl, 2005, Section 9.1.2 for the B-model). As a general remark, observe that constraining an element of  $B_t$  to be any constant other than zero is infeasible because all elements on the right hand side (RHS) of (3.5) are either zero or time varying due to the time-varying mixing weights.<sup>5</sup>

### 3.3 Maximum likelihood estimation

The parameters of the reduced form GMVAR model are collected to the vector  $\theta = (\vartheta_1, \dots, \vartheta_M, \alpha_1, \dots, \alpha_{M-1})$  ( $((M(d^2p+d+d(d+1)/2)+1) \times 1)$ , where  $\vartheta_m = (\phi_{m,0}, \text{vec}(A_{m,1}), \dots, \text{vec}(A_{m,p}), \text{vech}(\Omega_m))$ ,  $\text{vec}$  is a vectorization operator that stacks the columns of a matrix on top of each other, and  $\text{vech}$  stacks the columns of a matrix from the main diagonal downwards (including the main diagonal). The last mixing weight parameter  $\alpha_M$  is omitted because it is obtained from the constraint  $\sum_{m=1}^M \alpha_m = 1$ .

Using the notation described in Section 2, indexing the observed data as  $y_{-p+1}, \dots, y_0, y_1, \dots, y_T$ , and assuming that the initial values are stationary, the exact log-likelihood function of the reduced form GMVAR model takes the form (Kalliovirta et al., 2016, equations (9) and (10))

$$L_t(\theta) = \log \left( \sum_{m=1}^M \alpha_m n_{dp}(\mathbf{y}_0; \mathbf{1}_p \otimes \mu_m, \Sigma_m) \right) + \sum_{t=1}^T l_t(\theta), \quad (3.9)$$

where

$$l_t(\theta) = \log \left( \sum_{m=1}^M \alpha_{m,t} (2\pi)^{-d/2} \det(\Omega_m)^{-1/2} \exp \left\{ -\frac{1}{2} (y_t - \mu_{m,t})' \Omega_m^{-1} (y_t - \mu_{m,t}) \right\} \right). \quad (3.10)$$

If it does not seem reasonable to assume that the initial values  $\mathbf{y}_0 = (y_{-p+1}, \dots, y_0)$  are stationary, one may condition on them and base the estimation on the conditional log-likelihood function, which is obtained by dropping the first term on the RHS of (3.9).

The reduced form GMVAR model can be estimated by maximizing the exact or conditional likelihood function presented in (3.9) and (3.10) with respect to the parameter  $\theta$ . If  $M = 2$ , the

<sup>5</sup> We have focused on the B-model, where the structure is imposed on the contemporaneous relations of the shocks. Alternatively, one may consider the "A-model" setup in which the structure is placed on the contemporaneous relations of the observable variables governed by the "A-matrix" (see, e.g., Lütkepohl, 2005, Section 9.1.1). The A-model is obtained implicitly from the B-model (3.1) and (3.2) by defining the A-matrix as  $A_t \equiv B_t^{-1}$ , where  $B_t$  is given by (3.5). In this case, the structural model equation (3.1) becomes

$$A_t y_t = \sum_{m=1}^M (A_t \phi_{m,0} + \sum_{i=1}^p A_t A_{m,i} y_{t-i}) + e_t,$$

thereby incorporating continuously varying intercepts and coefficient matrices due to the constant covariance normalization of the structural shocks. In practice, however, one needs to carefully derive how any specific constraint on  $A_t$  can be imposed by restricting  $W$ .

structural GMVAR model is then obtained by simultaneously diagonalizing the error term covariance matrices as discussed Section 3.1. However, should overidentifying restrictions be imposed on  $B_t$  through  $W$  or if  $M \geq 3$ , it is more convenient to reparametrize the model with  $W$  and  $\Lambda_m$ ,  $m = 2, \dots, M$ , instead of  $\Omega_1, \dots, \Omega_M$  and maximize the log-likelihood function subject to the new set of parameters and constraints. In this case, the decomposition (3.4) is plugged in to the log-likelihood function and the  $\text{vech}(\Omega_1), \dots, \text{vech}(\Omega_M)$  are replaced with  $\text{vec}(W), \lambda_2, \dots, \lambda_M$ , where  $\lambda_m = (\lambda_{m1}, \dots, \lambda_{md})$ , in the parameter vector  $\theta$ .

Maximizing the complex and highly multimodal log-likelihood function can be challenging in practice, especially if there are more than two regimes. Following Dorsey and Mayer (1995), Meitz et al. (2018, 2021), and Virolainen (2021b,c), we employ a two-phase procedure where, in the first phase, a genetic algorithm is used to find starting values for a gradient based method which then, in the second phase, accurately converges to a nearby local maximum or saddle point. The genetic algorithm in the accompanying R package `gmvar` (Virolainen, 2021a) has been modified to improve its performance significantly, and it functions similarly to the one described in Virolainen (2021b) for the univariate GMAR (Kalliovirta et al., 2015), StMAR (Meitz et al., 2021), and G-StMAR (Virolainen, 2021b) models. In order to obtain reliable results, a (sometimes very large) number of estimation rounds should be performed, for which `gmvar` takes use of parallel computing.

## 4 Impulse response analysis

The expected effects of the structural shocks in the SGMVAR model generally depend on the initial values as well as on the sign and size of the shock, which makes the conventional way of calculating impulse responses unsuitable (see, e.g., Kilian and Lütkepohl, 2017, Chapter 4). Following Koop et al. (1996) and Kilian and Lütkepohl (2017, Section 18.2.2), we therefore consider the generalized impulse response function (GIRF) defined as

$$\text{GIRF}(n, \delta_j, \mathcal{F}_{t-1}) = \text{E}[y_{t+n} | \delta_j, \mathcal{F}_{t-1}] - \text{E}[y_{t+n} | \mathcal{F}_{t-1}], \quad (4.1)$$

where  $n$  is the chosen horizon and  $\mathcal{F}_{t-1} = \sigma\{y_{t-j}, j > 0\}$  as before. The first term on the RHS is the expected realization of the process at the time  $t + n$  conditionally on a structural shock of magnitude  $\delta_j \in \mathbb{R}$  in the  $j$ th element of  $e_t$  at the time  $t$  and the previous observations. The second term on the RHS is the expected realization of the process conditionally on the previous observations only. The GIRF thus expresses the expected difference in the future outcomes when the structural shock of magnitude  $\delta_j$  in the  $j$ th element hits the system at the time  $t$  as opposed to all shocks being random.

Due to the  $p$ -step Markov property of the SGMVAR model, conditioning on (the  $\sigma$ -algebra generated by) the  $p$  previous observations  $\mathbf{y}_{t-1} = (y_{t-1}, \dots, y_{t-p})$  is effectively the same as conditioning on  $\mathcal{F}_{t-1}$  at the time  $t$  and later. The history  $\mathbf{y}_{t-1}$  can be either fixed or random, but with random history the GIRF becomes a random vector, however. Using fixed  $\mathbf{y}_{t-1}$  makes sense when one is interested in the effects of the shock in a particular point of time, whereas more general results are obtained by assuming that  $\mathbf{y}_{t-1}$  follows the stationary distribution of the process. If one is,

on the other hand, interested in a specific regime,  $\mathbf{y}_{t-1}$  can be assumed to follow the stationary distribution of the corresponding component model.

The GIRF and its distributional properties can be approximated with a Monte Carlo algorithm that generates (partial) realizations of the process and then takes the sample mean for point estimate. If  $\mathbf{y}_{t-1}$  is random and follows the distribution  $G$ , the GIRF should be estimated for different values of  $\mathbf{y}_{t-1}$  generated from  $G$ , and then the sample mean and sample quantiles can be taken to obtain the point estimate and confidence intervals that reflect the uncertainty about the initial values. Such algorithm, which is adapted from Koop et al. (1996, pp. 135-136) and Kilian and Lütkepohl (2017, pp. 601-602), is given in Appendix B.

Because the SGMVAR model allows to associate specific features or economic interpretations to different regimes, it might be interesting to also examine the effects of a structural shock to the mixing weights  $\alpha_{m,t}$ ,  $m = 1, \dots, M$ . We then consider the related GIRFs

$$\text{GIRF}_\alpha(n, \delta_j, \mathcal{F}_{t-1}) = E[\alpha_{m,t+n} | \delta_j, \mathbf{y}_{t-1}] - E[\alpha_{m,t+n} | \mathbf{y}_{t-1}] \quad (4.2)$$

for which point estimates and confidence intervals can be constructed similarly to (4.1). Examination of the mixing weights' GIRFs may be of interest also because the asymmetries related to the sign and size of the shock are caused by the possibly resulting regime-switches.

## 5 Empirical application

As an empirical application, we study the potentially asymmetric effects of U.S. monetary policy shocks. Asymmetric effects of monetary policy shocks in the U.S. have been studied, among other, by Weise (1999), Garcia and Schaller (2002), Lo and Piger (2005), and Höppner et al. (2008), who all found the effects of monetary policy shocks to production stronger during recessions (or low growth periods) than booms (or high growth periods). Weise (1999) also found evidence supporting that large and small shocks have different effects, and that positive and negative monetary shocks have different effects when the shocks are large. Höppner et al. (2008) concluded that the real effects of monetary policy shocks seem to have decreased over their sample period from 1962 to 2002. Tenreyro and Thwaites (2016), on the other hand, found the effects of U.S. monetary policy shocks less powerful in recessions. Peersman and Smets (2002) found that monetary policy shocks have larger effects on production during recessions than expansions in the Euro area, while Burgard et al. (2019) found the effects of contractionary monetary policy shocks stronger but less enduring during "crisis" than during "normal times".

We consider the quarterly U.S. data covering the period from 1954Q3 to 2021Q1 (267 observations) and consisting of four variables: real GDP, GDP implicit price deflator, producer price index (all commodities), and an interest rate variable. Our policy variable is the interest rate variable, which is the effective federal funds (FF) rate from 1954Q3 to 2008Q2 after which we replaced it with the Wu and Xia (2016) shadow rate, which is not constrained by the zero lower bound and also quantifies unconventional monetary policy measures.<sup>6</sup> The Wu and Xia (2016) shadow rate

<sup>6</sup> The Federal Open Market Committee targeted the FF rate between 0.00-0.25 from December 2008 to December

data was retrieved from the Federal Reserve Bank of Atlanta’s website and the rest of the data was retrieved from the Federal Reserve Bank of St. Louis database.

The logarithms of real GDP, GDP deflator, and producer price index are clearly nonstationary (not shown) and hence need to be detrended before fitting a GMVAR model to the series. Some of the variables could be cointegrated, but due to the potential presence of structural breaks (for instance, in the Corona crisis), the possible cointegration vector may be time-varying. Since modelling (possibly time-varying) cointegration relations is beyond the scope of this paper, we treat the variables as if they are not cointegrated. We detrended the logarithm of real GDP by separating its cyclical component from the trend with one-sided Hodrick-Prescott (HP) filter and then considering the cyclical component.<sup>7</sup> We thereby assume that our monetary policy shocks do not have permanent effects on real output. We detrended the logarithms of the price variables by taking the first difference and then multiplying by hundred, so that the resulting series approximate the percentage growth rates. The interest rate variable is treated as stationary because the federal funds rate is controlled by the Fed who is expected keep it in a reasonable range.

The series are presented in the first four top panels of Figure 1 with the shaded areas indicating the periods of NBER based U.S. recessions. Throughout, we refer to the variables as  $GDP$  (output),  $GDPDEF$  (prices),  $PPI$  (commodity prices), and  $RATE$  (interest rate) without making it explicit that some of them are detrended. The (S)GMVAR model of autoregressive order  $p$  and  $M$  mixture components is referred to as (S)GMVAR( $p, M$ ) model.

We selected the order of our GMVAR model by first estimating a GMVAR(1, 2) model. Then, we increased the autoregressive order until the quantile residual autocorrelation test of Kalliovirta and Saikkonen (2010) passed at all the conventional levels of significance when taking into account four lags (accounting for one year). This led to a GMVAR(4, 2) model, which we found superior to its linear counterpart in terms of diagnostics and information criteria. Details on the model selection and quantile residual diagnostics are given in Appendix C.

The estimated mixing weights of the two regimes are presented in the bottom panel of Figure 1. The first regime (blue) dominates in the late 1950’s, then a period from late 1960’s to mid 1980’s, and finally again in the Corona crisis. We refer to this regime as *the unstable inflation regime*, as it generally exhibits high and volatile inflation. The second regime (red) prevails when the first one does not: mainly in the 1960’s and from the late 1980’s onwards but excluding the Corona crisis. We refer to this regime as *the stable inflation regime*. Details about the characteristics of the

---

2015 (and more recently from March 2020 onwards). However, because the Wu and Xia (2016) shadow rate is somewhat higher than the FF rate in 2008Q4, but the FF rate and the shadow rate are close to each other in 2008Q2 and 2008Q3, we replaced the FF rate with the shadow rate already in 2008Q3. This produces a transition between the two interest rates such that it does not introduce any artificial jumps to the combined interest rate variable.

<sup>7</sup> The one-sided filter was obtained from the two-sided HP filter by applying the filter up to horizon  $t$ , taking the last observation, and repeating this procedure for the full sample  $t = 1, \dots, T$ . In order to allow the series to start from any phase of the cycle, we applied the one-sided filter to the full available sample from 1947Q1 to 2021Q1 before extracting our sample period from it. We computed the two-sided HP filters with the R package `lpirfs` (Adämmer, 2021) by using the standard smoothing parameter value of 1600. For robustness, we also considered log-differencing and the linear projection filter proposed by Hamilton (2018). But they consistently led to generalized impulse responses where supposedly contractionary monetary policy shocks seemed to have considerable expansionary effects on GDP at least in one of the regimes (not shown). Hence, we preferred the HP filter.

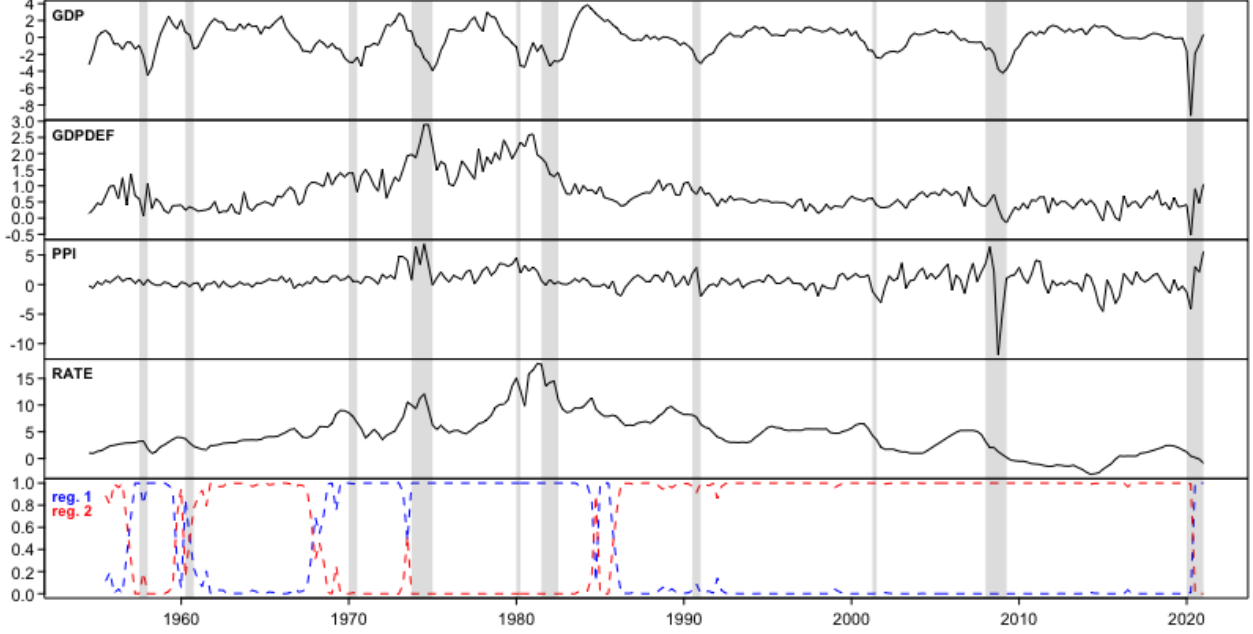


Figure 1: Quarterly U.S. series covering the period from 1954Q3 to 2021Q1. The top panel presents the cyclical component of real GDP (GDP) which we separated from the trend using the one-sided Hodrick-Prescott filter. The second and third panels the log-differences of GDP implicit price deflator (GDPDEF) and producer price index (PPI) multiplied by hundred. The fourth panel presents an interest rate variable which is the effective federal funds from 1954Q3 to 2008Q2 and the Wu and Xia (2016) shadow rate from 2008Q3 to 2021Q1. The bottom panel shows the estimated mixing weights of the fitted GMVAR(4, 2) model. The shaded areas indicate the NBER based U.S. recessions.

regimes are provided in Appendix C.

## 5.1 Identification of a monetary policy shock

Decomposing the covariance matrices of the reduced form GMVAR(4, 2) model as in (3.4) gives the following estimates for the structural parameters:

$$\hat{W} = \begin{bmatrix} \mathbf{0.02} (0.032) & -0.31 (0.094) & 1.22 (0.112) & -\mathbf{0.29} (0.286) \\ 0.03 (0.013) & 0.23 (0.023) & 0.17 (0.040) & -\mathbf{0.00} (0.051) \\ 1.01 (0.079) & \mathbf{0.09} (0.152) & 0.71 (0.126) & \mathbf{0.11} (0.198) \\ \mathbf{0.01} (0.017) & -\mathbf{0.02} (0.054) & 0.40 (0.158) & 1.04 (0.011) \end{bmatrix}, \hat{\lambda}_2 = \begin{bmatrix} 1.96 (0.372) \\ 0.42 (0.074) \\ 0.12 (0.022) \\ 0.06 (0.011) \end{bmatrix}, \quad (5.1)$$

where the ordering of the variables is  $y_t = (GDP_t, GDPDEF_t, PPI_t, RATE_t)$ , the estimates  $\hat{\lambda}_{2i}$  are in a decreasing order (which fixes an arbitrary ordering for the columns of  $\hat{W}$ ), and approximate standard errors are given in parentheses next to the estimates. The estimates that deviate from zero by less than two times their approximate standard error are bolded.

The shocks are statistically identified if all the  $\lambda_{2i}$ ,  $i = 1, \dots, 4$ , are different to each other. The

differences of the estimates are quite large relative to their standard errors, so inequality of the  $\lambda_{2i}$  seems plausible. But as already noted in Section 3.2, the standard errors are (asymptotically) valid only if the  $\lambda_{2i}$  parameters are different to each other in the first place, so we cannot make formal conclusions without considerably more complex examinations (see, e.g., Lütkepohl et al., 2021, for a related discussion). Nevertheless, in the absence of any apparent statistical or economic reason to believe that some of the  $\lambda_{2i}$  might be exactly equal to each other, we proceed by assuming that they are not.

Based on the estimates and their standard errors in (5.1), the first shock mainly moves commodity prices at impact, whereas the second shock moves production and inflation rate to opposite directions. Since the instantaneous movements of the interest rate variable are insignificant, these two shocks are not interesting monetary policy shock candidates. The third shock moves the interest rate significantly at impact, but since production and prices move significantly to the same direction, its characteristics appear similar to a demand shock rather than a monetary policy shock. The last shock moves the interest rate and production to opposite directions, while it also moves the inflation rate (insignificantly) to the opposite direction from interest rate and commodity prices to the same direction. Among the four structural shocks obtained for the model, the characteristics of the last shock thereby mostly resemble those of a monetary policy shock, so it is our monetary policy shock candidate.

Identifying a monetary policy shock with Proposition 2 requires such constraints to be imposed on  $W$  that it can be unambiguously distinguished from the other shocks. A common identification scheme is to place zero constraints on the instantaneous movements of production and prices, but this has been though as controversial in some of the literature (see, e.g., the discussions in Ramey, 2016, Section 3.3.1 and Uhlig, 2017, Section 3). Particularly with quarterly data, the zero constraints make the arguably implausible assumption that the aggregate economy does not react to an unexpected movement of the policy variable within three months. The zero instantaneous response may, nonetheless, be a useful approximation.

To study whether such constraints are consistent with the data, we test them with our model using a likelihood ratio test. Indexing  $W = [w_{ij}]_{i,j=1,\dots,4}$ , the likelihood ratio test for the zero-response of GDP,  $w_{14} = 0$ , obtains the  $p$ -value 0.331, while zero-response of inflation,  $w_{24} = 0$ , obtains the  $p$ -value 0.970, and the zero-response of commodity prices,  $w_{34} = 0$ , obtains the  $p$ -value 0.567. Testing the zero-response of inflation and commodity prices jointly,  $w_{24} = w_{34} = 0$ , gives the  $p$ -value 0.694. Testing all three zero constraints jointly,  $w_{14} = w_{24} = w_{34} = 0$ , gives the  $p$ -value 0.099, but testing the additional zero constraint on GDP conditional the zero constraints on both prices gives the  $p$ -value 0.019. That is, all the three conventional zero constraints are accepted both individually and jointly, but imposing additional zero constraint on the output when the instantaneous movements of prices are constrained zero is rejected at 5% level of significance.<sup>8</sup>

Because the estimated sign of the instantaneous movement of output is economically plausible (it states that increasing interest rate unexpectedly decreases economic activity within three months) and all the tests accepted zero constraints on prices, we consider zero constraints on the prices only. Since also the sign of the instantaneous response of the inflation rate is plausible (it states

<sup>8</sup> Wald test produces similar results (not shown).

that increasing interest rate unexpectedly decreases inflation<sup>9</sup>), we consider an identification that imposes these sign constraints. In addition, we place a zero constraint on the instantaneous response of commodity prices, as it allows to formally identify the monetary policy shock without imposing restrictive constraints on the other shocks.

Our identifying constraints are summarized in  $W_1$  in (5.2), where the last column is for the monetary policy shock. Our identification is not very restrictive on the other three shocks: it merely assumes that two of shocks move commodity prices at impact and the third one moves output and prices to opposite directions. The latter assumption is plausible, because it characterizes what can be expected from a supply shock. These assumptions are also supported by the magnitude of the estimates relative to their standard errors given in (5.1).

$$W_1 = \begin{bmatrix} * & - & * & - \\ * & + & * & - \\ + & * & + & 0 \\ * & * & * & + \end{bmatrix}, \quad W_2 = \begin{bmatrix} * & * & * & - \\ * & + & * & 0 \\ + & * & + & 0 \\ * & * & * & + \end{bmatrix} \quad (5.2)$$

Condition (2) of Proposition 2 is satisfied because the first and third columns of  $W_1$  cannot satisfy the zero constraint in the last column due to the strict sign constraints, and the second column with the opposite sign constraints cannot satisfy the same sign constraints in the first two elements of the last column. Validity of condition (1) was assumed and condition (3) is satisfied, as there is at least one strict sign constraint in the last column of  $W_1$ . Therefore, the last shock is identified.

If one is unwilling to impose any restrictive sign constraints on the first three shocks, also the instantaneous response of inflation to monetary policy shock can be constrained to zero. Conditionally on the zero constraint on commodity prices only, likelihood ratio test accepts the second zero constraint with the  $p$ -value 0.694 (and Wald test with  $p$ -value 0.524). In this case, it suffices to assume that among the first three shocks, there are two shocks that move commodity prices at impact and that the third one moves the inflation rate at impact. Again, the estimates and approximate standard errors in (5.1) show that these assumptions are statistically plausible, while they are not very restrictive either. These identifying constraints are summarized in  $W_2$  in (5.2).

Since the monetary policy shock is still identified when the strict sign constraint for inflation rate in the last column of  $W_1$  is relaxed to a non-strict sign constraint, and using non-strict sign constraint is less restrictive than using a zero constraint, we prefer the identification in  $W_1$  but with the non-strict sign constraint.<sup>10</sup> The estimates are given in (5.3) with the approximate standard errors in parentheses next to the estimates. Compared to the unrestricted estimates (5.1), the negative instantaneous response of GDP became larger and statistically significant. Also the negative instantaneous response of inflation rate became larger, but it remains small relative to its standard error.

<sup>9</sup> The prices decrease as a result of decreased demand. The prices could also rise as result of decreased supply, however, which we briefly discuss in Section 5.2

<sup>10</sup>Using the constraints in  $W_2$  does not, however, change the generalized impulse responses much (not shown).

$$\hat{W}_1 = \begin{bmatrix} \mathbf{0.01} (0.032) & -0.31 (0.093) & 1.19 (0.108) & -0.42 (0.165) \\ 0.03 (0.013) & 0.23 (0.023) & 0.17 (0.040) & \mathbf{-0.02} (0.035) \\ 1.01 (0.079) & \mathbf{0.09} (0.153) & 0.72 (0.126) & 0 \\ \mathbf{0.02} (0.017) & \mathbf{-0.02} (0.054) & 0.47 (0.102) & 0.99 (0.097) \end{bmatrix}, \hat{\lambda}_2 = \begin{bmatrix} 1.96 (0.371) \\ 0.42 (0.074) \\ 0.12 (0.022) \\ 0.06 (0.011) \end{bmatrix}, \quad (5.3)$$

Finally, observe that according Proposition 2, the monetary policy shock is still identified if  $\lambda_{21} = \lambda_{22} = \lambda_{23}$ . By Proposition 3, with the constraints in  $W_1$  the monetary policy shock is identified even if additionally  $\lambda_{21} = \lambda_{24}$  or  $\lambda_{23} = \lambda_{24}$ . With the constraint in  $W_2$ , the shock is identified also if  $\lambda_{22} = \lambda_{24}$ . Thus, our identification of the monetary policy shock is not very sensitive to the validity of Assumption 1.

## 5.2 Generalized impulse response functions

Due to the endogenously determined regime-switching probabilities and the fact that we allow the regime to switch as a result of a shock, there are multiple types of possible asymmetries: the impulse responses can vary depending on the initial value and the sign and size of the shock. We study the state-dependence of the (generalized) impulse responses by drawing initial values from the stationary distribution of each regime separately. Then, we calculate the 95% confidence intervals that reflect uncertainty about the initial value within the given regime as is described in Section 4 and Appendix B. Asymmetries related to the sign and size of the shock are studied by estimating the GIRFs for positive (contractionary) and negative (expansive) one-standard-error (small) and two-standard-error (large) shocks. All GIRFs are scaled so that the peak effect of the interest variable is 100 basis points within the first four quarters, making the responses to shocks of different sign and size comparable.

Figure 2 presents the GIRFs  $N = 0, 1, \dots, 32$  quarters ahead estimated for the identified monetary policy shock using  $R_1 = R_2 = 2500$  in the Monte Carlo algorithm. The GIRFs of inflation rate and commodity price inflation rate are not accumulated to levels. From the top to bottom, the responses of GDP, inflation rate, commodity price inflation rate, interest rate, and the first regime's mixing weights are depicted in each row, respectively. The first [second] column shows the responses to positive (blue solid line) and negative (red dashed line) one-standard-error shocks with the initial values generated from the stationary distribution of the first [second] regime. The third [fourth] column shows the responses to positive and negative two-standard-error shocks with the initial values generated from the first [second] regime. The shaded areas represent the 95% confidence intervals that reflect uncertainty about the initial value within the given regime. Responses of the second regime's mixing weights are omitted because they are the negative of the first regime's mixing weights' responses.

In the first regime (the unstable inflation regime), contractionary (expansive) monetary policy shock induces a strong contraction (expansion) to the cyclical component of GDP, with the peak effect occurring after two to three quarters. After roughly two years, from most of the starting

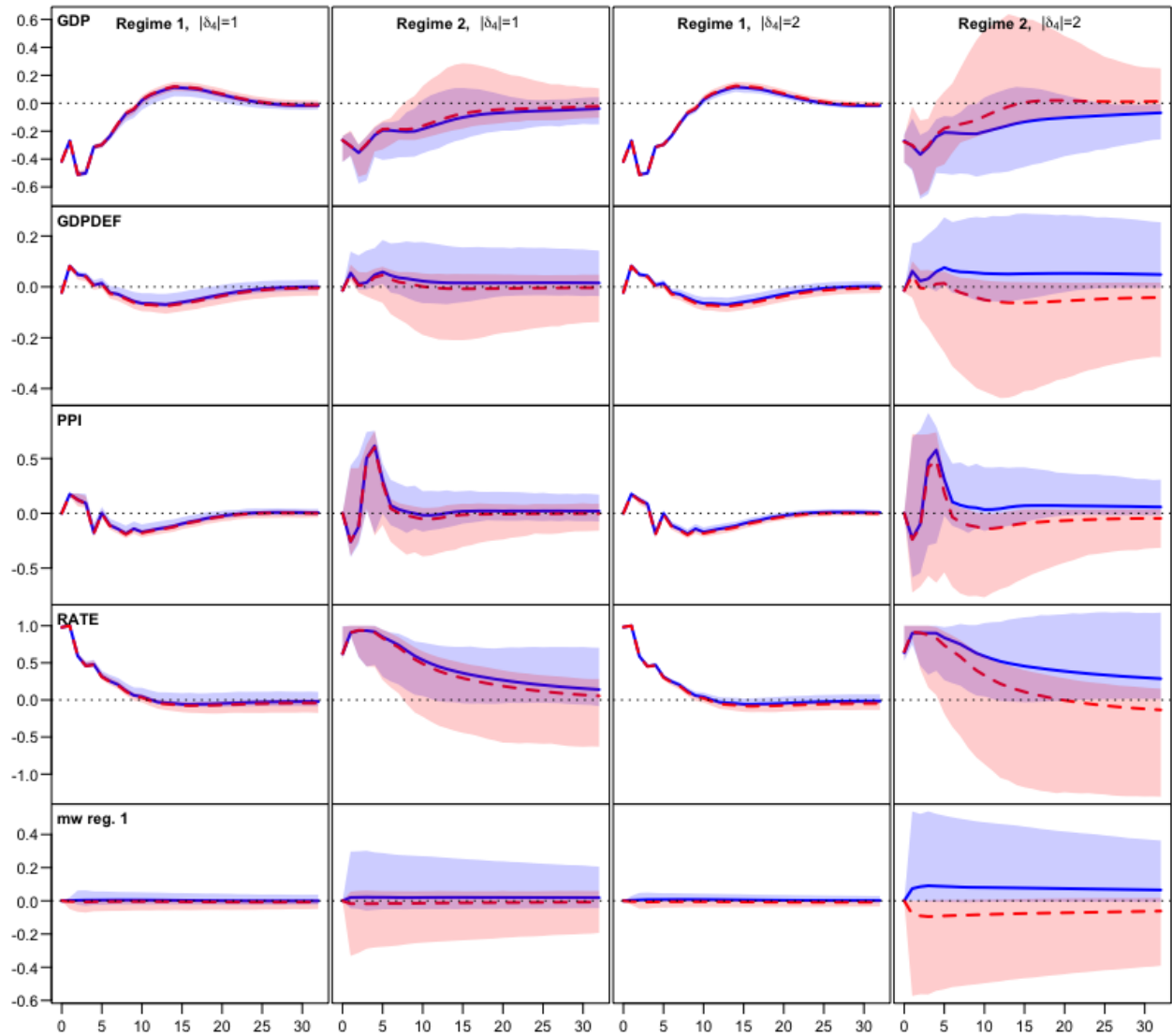


Figure 2: Generalized impulse response functions  $N = 0, 1, \dots, 32$  quarters ahead estimated for the monetary policy shock identified in Section 5.1 using  $R_1 = R_2 = 2500$  in the Monte Carlo algorithm presented in Appendix B. From the top to bottom, the responses of production, prices, commodity prices, the interest rate variable, and the first regime's mixing weights are depicted in each row, respectively. The GIRFs are not accumulated for the prices variables, i.e., to responses are for inflation rates. The first [second] column shows the responses to a positive (blue solid line) and negative (red dashed line) one-standard-error shocks with the initial values generated from the stationary distribution of the first [second] regime. The third [fourth] column shows the responses to a positive and negative two-standard-error shocks with the initial values generated from the first [second] regime. All GIRFs have been scaled so that peak effect of the interest rate variable is 100 basis points during the first four quarters. The shaded areas represent the 95% confidence intervals that reflect uncertainty about the initial state within the given regime. Responses of the second regime's mixing weights are omitted because they are the negative of the first regime's mixing weights' responses.

values the response becomes expansive (contractionary) before decaying to zero.<sup>11</sup> Inflation rate and commodity price inflation rate rise after the impact and then decrease significantly for several years before the price levels stabilize. The short-term increase in the inflation is possibly due to a cost-push effect of the monetary policy shock, which was also observed by Barth and Ramey (2001), for instance (the cost side effects of monetary policy shocks are discussed in more detail in relation to the second regime's GIRFs). The interest rate decays towards zero for roughly two years after which, on average, it decreases slightly below (above) zero before returning to zero.

The response of the interest rate switches its sign less significantly when the shock is contractionary, when also the inflationary effects of the shock are slightly weaker. It thereby seems that the interest rate falls (rises) as an endogenous response to stabilize the price level, in part causing the delayed expansion (contraction) in GDP before decaying to zero. Based on the slightly narrower confidence bounds, the delayed expansion (contraction) in GDP and the inflationary effects are slightly more significant when the shock is large, but the shapes of the impulse responses are similar for small and large shocks.

In the second regime (the stable inflation regime), contractionary (expansive) monetary policy shock induces a significant contraction (expansion) to GDP, with the peak effect occurring after two quarters. On average, the GDP decays relatively slowly towards zero, but similarly to the first regime, it switches sign from some of the starting values. Particularly large expansive shocks seem to cause a strong contraction from some of the starting values roughly after two years from impact.

The prices seem to mostly rise as a response to a contractionary monetary policy shock, although one would often expect contractionary monetary policy shocks to decrease inflation due to the decreased demand. Aggregate demand decreases, because in a sticky price environment the increase of nominal interest rate leads to an increase of real interest rate, and thereby to postponed consumption (see, e.g., Galí, 2015, for a new Keynesian model incorporating such dynamics). This is referred to as the demand channel.<sup>12</sup>

Prices rising as a result of a contractionary monetary policy shock is often referred to as *prize puzzle*, and it has been discussed recently, for instance, in Ramey (2016, Section 3.3.2, and the references therein). One explanation is that the Fed uses more information in predicting the future inflation than the past of the variables included in the VAR. Consequently, the identified monetary policy shock also contains a component that incorporates the Fed's endogenous response to the prediction of the future inflation that is not captured by the past of the included variables.

Another explanation to the prize puzzle proposes that since rising interest rate increases the cost of working capital, the cost of production is increased and thereby firms may find it optimal to reduce the supply. The reduction in supply, in turn, then increases the price level. This is referred to as the cost channel (e.g., Barth and Ramey, 2001, see Ravenna and Walsh, 2006, for a new Keynesian model incorporating the cost channel). If the cost channel is more dominant than the demand channel, prices increase as a response to a contractionary monetary policy shock. If the

---

<sup>11</sup>By zero, we mean the expected observation if all the shocks were random.

<sup>12</sup>There are also multiple other monetary transmission mechanisms proposed in the literature. Many of them are summarized in Mishkin (1996), for instance. We refer to the monetary transmission mechanisms that affect real economic activity through changing the aggregate demand generally as the demand channel.

demand channel is more dominant, prices decrease (see Rehman, 2014, 2015, for an illustration). But if the identified monetary policy shock incorporates a significant endogenous component, it is difficult to say how much we can infer about the dominance of demand and cost channels at a given point time based on the generalized impulse response functions. Because there are only 267 observations in the series (and less than that from each regime), some of the possibly implausible movements of the variables may also be attributed to an estimation error.

Despite of whether the arguably unexpected movements of prices are caused by the dominating cost channel or endogeneity of the shock (or both), given the movements of the prices, the endogenous movements of the variables seem reasonable.<sup>13</sup> When the prices rise as a response to a contractionary monetary policy shock (the second and fourth columns in Figure 2), the interest rate stays high persistently, and it is accompanied with a persistent contraction in real economic activity.<sup>14</sup> This is illustrated in Figure 6 in Appendix C.3, which presents 200 unscaled GIRFs of one-standard-error (left panels) and two-standard-error (right panels) contractionary monetary policy shocks with the starting values generated from the second regime. The GIRFs that incorporate quarterly inflation of at least 0.1% for one-standard-error shocks or 0.25% for two-standard-errors shocks are coloured red and the rest black. As the Figure shows, the GIRFs that exhibit high inflation (red) are the ones that also exhibit high interest rate and persistent contraction in the GDP, while the GIRFs exhibiting low or no inflation (black) exhibit lower interest rate and weaker contraction in the GDP. The GIRFs of the first regime's mixing weights show that the high inflation and persistent contraction are due to the higher probability of entering the unstable inflation regime.

On average, the inflation does not move much as a response to a small expansionary monetary policy shock (the second column in Figure 2), while the interest rate stays low relatively persistently, causing the relatively persistent expansion in the GDP. The delayed contraction from some of the starting values is related to the sample paths associated with high inflation and thereby increased interest rate, when the Fed's response to the inflation is tight monetary policy. This is illustrated in Figure 6 in Appendix C.3 (left panels), which presents 200 unscaled GIRFs of one-standard-error expansionary monetary policy shocks. The GIRFs that incorporate quarterly inflation of at least 0.1% are coloured red and the rest are black. Similarly to the contractionary shock, the high inflation from some of the starting values is related to the higher probability of entering the unstable inflation regime.

Large expansionary shocks (the fourth column in Figure 2) drive the economy towards the unstable inflation regime relatively more than small expansionary shocks. Prices increase and the interest rate increases relatively fast towards zero, and from some of the starting values it increases much higher than that. The high interest rate then appears to cause the strong contraction in the GDP

---

<sup>13</sup>If the movements of some variables are not sensible, the endogenous movements of the other variables that are effected by the non-sensible movements can be questioned. Nonetheless, we find our empirical results interesting, as there exists a logical explanation to the price puzzle through the cost channel effect of monetary policy, and the price puzzle arises only from some of the starting values, while its occurrence is also sensitive to the sign and size of the shock. Moreover, since our model uniquely identifies the B-matrix up to changing the ordering of the columns and all signs in a column, one of its columns unambiguously characterize the estimated effects of a monetary policy shock (as long as the assumption of a single B-matrix is accepted). The identifying constraints in Section 5.1, in turn, formally ensure that the correct column is chosen despite of the estimation error.

<sup>14</sup>Even if raising the interest rate unexpectedly actually raises prices through the cost channel, it makes sense that the interest stays high persistently if the Fed's endogenous response to high inflation is tight monetary policy.

that quickly follows the initial short-term expansion. The right panels of Figure 6 in Appendix C.3 present 200 GIRFs of two-standard-error expansionary shocks with the ones incorporating quarterly inflation of at least 0.25% coloured red. As the figure shows, the GIRFs exhibiting the strong delayed contraction are the ones that also exhibit high inflation and high interest rate together with significantly increased probability of entering the unstable inflation regime.

Overall, expansionary and contractionary monetary policy shocks seem to both increase the probability of the unstable inflation regime, significantly more so if the economy is in the stable regime when the shock hits (the bottom panels in Figure 2). Also, large shocks in the stable inflation regime increase the probability of the unstable regime relatively more than small shocks. Because contractionary shocks generally increase inflation in the stable inflation regime, while expansionary shocks also increase inflation or do not move it much, it appears that the cost channel effect of monetary policy shocks might be more dominant for contractionary than expansionary shocks - but only in the stable inflation regime.

Another interesting observation from our model is that it implies that in 2021Q1, we are in the same unstable inflation regime where we were in the 1970's, when the U.S. economy suffered from stagflation. Our model exhibits the switch from the stable inflation regime to the unstable inflation regime in the beginning of the Corona crisis, with the switch happening between the first and second quarter of 2020 with probability of approximately 0.01 and between second and third quarter with probability of practically one (assuming the switch did not happen in the previous period). Given our results on how large expansionary monetary policy shocks propagate to higher probability of the unstable inflation regime in the period after the impact, it could be that the Fed's very expansionary monetary policy in the beginning and during the Corona crisis is related to the switch.

## 6 Summary

We introduced a structural version of the Gaussian mixture vector autoregressive model (Kalliovirta et al., 2016) that incorporates endogenously determined mixing weights and a time-varying B-matrix. We showed that our model generally identifies the structural shocks up to ordering and sign, but does not reveal which column of the B-matrix is related to which shock. Since the B-matrix is also subject to an estimation error, we took use of the matrix decomposition proposed by Lanne and Lütkepohl (2010) and Lanne et al. (2010) and derived general conditions for formally identifying any subset of the shocks. This led to more flexible identification conditions than in the conventional SVAR models, while some of the constraints are also testable. For impulse response analysis, we utilized the generalized impulse response function (Koop et al., 1996) and proposed a Monte Carlo algorithm for its estimation by taking use of the known stationary distribution of the SGMVAR process.

The empirical application studied asymmetries in the expected effects of monetary policy shocks in the U.S. using a quarterly series covering the period from 1954Q3 to 2021Q1. Our SGMVAR model identified two regimes: a stable inflation regime and an unstable inflation regime, which dominates in the late 1950's, in the 1970's and early 1980's, and recently in the Corona crisis.

We found the effects of monetary policy shocks relatively symmetric in the unstable inflation regime, as they rarely cause a switch to the stable inflation regime. A contractionary (expansionary) monetary policy shock appears to first increase (decrease) inflation, possibly through short-term cost-push effect. Then, the inflation significantly decreases (increases) for several years. The strong contraction (expansion) in the cyclical component of GDP lasts for roughly two years and is followed by a short-term expansion.

The effects of monetary policy shocks were found strongly asymmetric in the stable inflation regime. Large shocks often induce relatively stronger inflationary effects, while both contractionary and expansionary shocks seem to increase inflation by driving the economy towards the unstable inflation regime. This suggests that in the stable inflation regime, the cost side effects of monetary policy shocks might be more dominant for contractionary than expansionary shocks. We also found that particularly large expansionary shocks often propagate to significantly higher probability of the unstable inflation regime and high inflation, which results in increasing interest rate and a strong contraction to the GDP after the initial short-term expansion.

## References

- Adämmer, P. (2021). *lpirfs: Local Projections Impulse Response Functions*. R package version: 0.2.0.
- Barth, M. J. and Ramey, V. A. (2001). The cost channel of monetary transmission. In Bernanke, B. S. and Rogoff, K., editors, *NBER Macroeconomics Annual*, volume 16, pages 199—239. MIT Press, Cambridge.
- Bentarzi, M. and Djeddou, L. (2014). On mixture periodic vector autoregressive models. *Communications in Statistics - Simulation and Computation*, 43(10):2325–2352.
- Burgard, J., Neuenkirch, M., and Nöckel, M. (2019). State-dependent transmission of monetary policy in the euro area. *Journal of Money, Credit and Banking*, 51(7):2053–2070.
- Dorsey, R. and Mayer, W. (1995). Genetic algorithms for estimation problems with multiple optima, nondifferentiability, and other irregular features. *Journal of Business and Economic Statistics*, 13(1):53–66.
- Fong, P., Li, W., Yau, C., and Wong, C. (2010). On a mixture vector autoregressive model. *The Canadian Journal of Statistics*, 35(1):135–150.
- Galí, J. (2015). *Monetary Policy, Inflation, and the Business Cycle*. Princeton University Press, Princeton and Oxford, 2nd edition.
- Garcia, R. and Schaller, H. (2002). Are the effects of monetary policy asymmetric? *Economic Inquiry*, 40(1):102–119.
- Hamilton, J. D. (2018). Why you should never use the hodrick-prescott filter. *The Review of Economics and Statistics*, 100(5):831–843.

- Höppner, F., Melzer, C., and Neumann, T. (2008). Changing effects of monetary policy in the us – evidence from a time-varying coefficient var. *Applied Economics*, 40(18):2353–2360.
- Kalliovirta, L. (2012). Misspecification tests based on quantile residuals. *The Econometrics Journal*, 15(2):358–393.
- Kalliovirta, L., Meitz, M., and Saikkonen, P. (2015). A gaussian mixture autoregressive model for univariate time series. *Journal of Time Series Analysis*, 36(2):247–266.
- Kalliovirta, L., Meitz, M., and Saikkonen, P. (2016). Gaussian mixture vector autoregression. *Journal of Econometrics*, 192(2):465–498.
- Kalliovirta, L. and Saikkonen, P. (2010). Reliable residuals for multivariate nonlinear time series models. *Unpublished revision of HECER discussion paper No. 247*.
- Kilian, L. and Lütkepohl, H. (2017). *Structural Vector Autoregressive Analysis*. Cambridge University Press, Cambridge, 1st edition.
- Koop, G., Pesaran, M., and Potter, S. (1996). Impulse response analysis in nonlinear multivariate models. *Journal of Econometrics*, 74(1):119–147.
- Lanne, M. and Lütkepohl, H. (2010). Structural vector autoregressions with nonnormal residuals. *Journal of Business & Economic Statistics*, 28(1):159–168.
- Lanne, M., Lütkepohl, H., and Maciejowska, K. (2010). Structural vector autoregressions with markov switching. *Journal of Economic Dynamics and Control*, 34(2):121–131.
- Lo, M. and Piger, J. (2005). Is the response of output to monetary policy asymmetric? evidence from a regime-switching coefficients model. *Journal of Money, Credit and Banking*, 37(5):865–886.
- Lütkepohl, H. (2005). *New Introduction to Multiple Time Series Analysis*. Springer, Berlin, 1st edition.
- Lütkepohl, H., Meitz, M., Netšunajev, A., and Saikkonen, P. (2021). Testing identification via heteroskedasticity in structural vector autoregressive models. *The Econometrics Journal*, 24(1):1–22.
- Meitz, M., Preve, D., and Saikkonen, P. (2018). *StMAR Toolbox: A MATLAB Toolbox for Student's t Mixture Autoregressive Models*.
- Meitz, M., Preve, D., and Saikkonen, P. (2021). A mixture autoregressive model based on student's *t*-distribution. *Communications in Statistics - Theory and Methods*.
- Meitz, M. and Saikkonen, P. (2021). Testing for observation-dependent regime switching in mixture autoregressive models. *Journal of Econometrics*, 222(1):601–624.
- Mishkin, F. S. (1996). The channels of monetary transmission: lessons for monetary policy. Working Paper 5464, National Bureau of Economic Research.

- Muirhead, R. (1982). *Aspects of Multivariate Statistical Theory*. John Wiley & Sons, Hoboken, New Jersey, 1st edition.
- Peersman, G. and Smets, F. (2002). Are the effects of monetary policy in the euro area greater in recessions than in booms? In Mahadeva, L. and Sinclair, P., editors, *Monetary Transmission in Diverse Economies*, pages 28–48. Cambridge University Press.
- Ramey, V. A. (2016). Macroeconomic shocks and their propagation. In Taylor, J. B. and Uhlig, H., editors, *Handbook of Macroeconomics*, volume 2, chapter 2. Elsevier Science B.V.
- Ravenna, F. and Walsh, C. E. (2006). Optimal monetary policy with the cost channel. *Journal of Monetary Economics*, 53(2):199–216.
- Rehman, A. U. (2014). Relationship between energy prices, monetary policy and inflation; a case study of south asian economies. *Journal of Central Banking Theory and Practice*, 3(1):43–58.
- Rehman, A. U. (2015). Revival of legacy of tooke and gibson: Implications for monetary policy. *Journal of Central Banking Theory and Practice*, 4(2):37–58.
- Tenreiro, S. and Thwaites, G. (2016). Pushing on a string: Us monetary policy is less powerful in recessions. *American Economic Journal: Macroeconomics*, 8(4):43–74.
- Uhlig, H. (2017). Shocks, sign restrictions, and identification. In Honoré, B., Pakes, A., Piazzesi, M., and Samuelson, L., editors, *Advances in Economics and Econometrics*, volume 2, chapter 4. Cambridge University Press.
- Virolainen, S. (2021a). *gmvarKit: Estimate Gaussian Mixture Vector Autoregressive Model*. R package version 2.0.0, available at CRAN: <https://CRAN.R-project.org/package=gmvarKit>.
- Virolainen, S. (2021b). A mixture autoregressive model based on gaussian and student's  $t$ -distributions. *Studies in Nonlinear Dynamics & Econometrics*.
- Virolainen, S. (2021c). *uGMAR: Estimate Univariate Gaussian or Student's  $t$  Mixture Autoregressive Model*. R package version 3.4.0.
- Weise, C. (1999). The asymmetric effects of monetary policy: A nonlinear vector autoregression approach. *Journal of Money, Credit and Banking*, 31(1):85–108.
- Wu, J. and Xia, F. (2016). Measuring the macroeconomic impact of monetary policy at the zero lower bound. *Journal of Money, Credit and Banking*, 48(2-3):253–291.

# Appendix A Proofs

## A.1 Proof of Lemma 1

Consider  $M$  positive definite  $(d \times d)$  covariance matrices  $\Omega_m$ ,  $m = 1, \dots, M$  and suppose  $B$  is any invertible  $(d \times d)$  matrix such that  $B^{-1}\Omega_m B'^{-1}$  are diagonal matrices with strictly positive diagonal entries. It follows that  $B^{-1}\Omega_1 B'^{-1} = \Lambda_m^{-1} B^{-1}\Omega_m B'^{-1}$  for some  $(d \times d)$  diagonal matrices  $\Lambda_m^{-1}$ ,  $m = 2, \dots, M$ , that have strictly positive diagonal entries. Elementary matrix algebra then shows that these identities are equivalent to  $B\Lambda_m = \Omega_m\Omega_1^{-1}B$ ,  $m = 2, \dots, M$ . Thus, the matrices  $B$  and  $\Lambda_m$  solve the eigenvalue problem of  $\Omega_m\Omega_1^{-1}$  with the diagonal of  $\Lambda_m = \text{diag}(\lambda_{m1}, \dots, \lambda_{md})$  containing the strictly positive eigenvalues and the columns of  $B$  being the related eigenvectors. Since this holds for any invertible  $(d \times d)$  matrix  $B$  that simultaneously diagonalizes the covariance matrices, it is also a necessary property of a time-varying B-matrix  $B_t$ .

Suppose also  $BA$  solves the eigenvalue problems of  $\Omega_m\Omega_1^{-1}$ ,  $m = 2, \dots, M$ , for some invertible  $(d \times d)$  matrix  $A$ . That is,  $BA\Lambda_m = \Omega_m\Omega_1^{-1}BA$  which is equivalent to  $A\Lambda_m A^{-1} = B^{-1}\Omega_m\Omega_1^{-1}B$ . But since  $B^{-1}\Omega_m\Omega_1^{-1}B = \Lambda_m$ , this implies that  $A\Lambda_m A^{-1} = \Lambda_m$ , which is equivalent to  $A\Lambda_m = \Lambda_m A$ . Thus,  $\lambda_{mi}a_{ij} = \lambda_{mj}a_{ij}$  where  $a_{ij}$  is the  $ij$ th element of  $A$ . It follows that  $a_{ij} = 0$  if  $\lambda_{mi} \neq \lambda_{mj}$  for some  $m$ , implying that  $A$  is diagonal matrix under Assumption 1, and  $BA$  multiplies each of the columns of  $B$  by a scalar. It is well known that eigenvalues of a matrix are unique (up to order), but since the diagonal elements of  $\Lambda_m$  can be in any order, so can the related eigenvectors that are the columns of  $B$ . That is,  $B$  is unique up to scalar multiples and ordering of its columns. Since the above holds for any appropriate B-matrices  $B$  and  $BA$ , it holds also for a time-varying B-matrix  $B_t$  at each  $t$ . ■

## A.2 Proof of Proposition 1

Lemma 1 shows that the B-matrix  $B_t$  is unique up to scalar multiples and reordering of its columns. Suppose the conditional covariance matrix of the structural error is normalized to a constant diagonal matrix with strictly positive diagonal entries, say  $C$ . That is,  $\sum_{m=1}^M \alpha_{m,t} B_t^{-1} \Omega_m B_t'^{-1} = C$ , which is equivalent to  $\sum_{m=1}^M \alpha_{m,t} \Omega_m = B_t C B_t'$ . Suppose that this identity also holds with another B-matrix,  $B_t E_t$ , where  $E_t$  is a possibly time-varying, invertible  $(d \times d)$  matrix. We have  $\sum_{m=1}^M \alpha_{m,t} (B_t E_t)^{-1} \Omega_m (B_t E_t)'^{-1} = C$ , which is equivalent to  $\sum_{m=1}^M \alpha_{m,t} \Omega_m = (B_t E_t) C (B_t E_t)'$ . Thus,  $B_t C B_t' = (B_t E_t) C (B_t E_t)'$ . By Lemma 1, the B-matrix is unique up to scalar multiples and reordering of its columns, so with a given ordering of the columns,  $E_t$  is a diagonal matrix. It then follows from  $B_t C B_t' = (B_t E_t) C (B_t E_t)'$  that  $C = E_t C E_t$ , which in turn implies  $c_i = e_{t,i}^2 c_i$ , where  $c_i$  and  $e_{t,i}$  are the  $i$ th diagonal elements of  $C$  and  $E_t$ , respectively. Therefore,  $e_{t,i} = \pm 1$ , implying that with a given ordering of the columns, (for each  $t$ )  $B_t$  is unique up to changing all signs in a column. Therefore,  $B_t$  is unique up ordering of its columns and changing all signs in a column. ■

### A.3 Proof of Proposition 2

Let  $\Omega_1, \dots, \Omega_M$  be positive definite covariance matrices. We consider the decomposition  $\Omega_1 = WW'$  and  $\Omega_m = W\Lambda_m W'$ ,  $m = 2, \dots, M$ , where  $\Lambda_m = \text{diag}(\lambda_{m1}, \dots, \lambda_{md})$ ,  $\lambda_{mi} > 0$  ( $i = 1, \dots, d$ ), contains the eigenvalues of  $\Omega_m \Omega_1^{-1}$  in the diagonal and the columns of the nonsingular  $W$  are the related eigenvectors. The decomposition always exists when  $M = 2$  (see, e.g., Muirhead, 1982, Theorem A9.9) but not necessarily when  $M \geq 3$ . In the following, we assume the covariance matrices satisfy the decomposition.

Repeating some of the proof in Lanne et al. (2010, p. 130, see also the proof of Theorem A9.9 in Muirhead, 1982) for convenience, suppose that we also have  $\Omega_1 = DD'$  and  $\Omega_m = D\Lambda_m D'$ ,  $m = 2, \dots, M$ , for some nonsingular ( $d \times d$ ) matrix  $D$ . Because  $D^{-1}WW'D'^{-1} = D^{-1}\Omega_1 D'^{-1} = I_d$ , the matrix  $Q' \equiv D^{-1}W$  is orthogonal, and hence,  $D = WQ$  and  $\Lambda_m Q = Q\Lambda_m$ . It follows that  $\lambda_{mi}q_{ij} = \lambda_{mj}q_{ij}$  where  $q_{ij}$  is the  $ij$ th element of  $Q$ . Thus,  $q_{ij} = 0$  if  $\lambda_{mi} \neq \lambda_{mj}$  for some  $m$ . Assuming that this (condition (1)) is satisfied by the last  $d_1 \in \{1, \dots, d\}$  eigenvalues, it follows that  $Q$  is a block-diagonal matrix with two blocks in the diagonal. Denoting  $d_0 \equiv d - d_1$ , the first block is a  $(d_0 \times d_0)$  matrix and the second one is a  $(d_1 \times d_1)$  diagonal matrix with  $q_{d_0+1, d_0+1}, \dots, q_{d, d}$  in the diagonal (if  $d_1 = d$ ,  $Q$  simply reduces to a diagonal matrix).

As the blocks in the diagonal of an orthogonal block-diagonal matrix are orthogonal and the eigenvalues of a diagonal real orthogonal matrix are  $\pm 1$ , it follows that the eigenvalues of the second block in the diagonal of  $Q$  are  $\pm 1$ . Then, because the eigenvalues of a block-diagonal matrix are the eigenvalues of the blocks in the diagonal, and eigenvalues of a diagonal matrix are its diagonal elements, it must be that  $q_{d_0+1, d_0+1}, \dots, q_{d, d}$  are  $\pm 1$ .

Thus, because  $D = WQ$ , the last  $d_1$  columns of  $W$  are unique up to changing all signs in a column, for given  $\Lambda_m$ ,  $m = 2, \dots, M$ . Since  $\Lambda_m$  are unique up to ordering of the diagonal elements and condition (2) fixes a unique ordering for the last  $d_1$  columns of  $W$  and hence also for the related eigenvalues  $\lambda_{mi}$ ,  $i > d_0$ , the last  $d_1$  columns of the B-matrix (3.5) are uniquely identified up to changing all signs in a column. Finally, condition (3) fixes the signs in the last  $d_1$  columns of  $W$  and consequently of  $B_t$ , implying that the last  $d_1$  columns of the B-matrix are (globally) unique for given mixing weights  $\alpha_{1,t}, \dots, \alpha_{M,t}$ . Moreover, if  $d_1 = d$ , the decomposition (3.4) of  $\Omega_1, \dots, \Omega_M$  is (globally) unique. ■

### A.4 Proof of Proposition 3

Consider the matrix decomposition of  $\Omega_m$ ,  $m = 1, \dots, M$  of Proposition 2. It is shown in the proof of Proposition 2 that any  $(d \times d)$  matrix  $D$  that also satisfies  $\Omega_1 = DD'$  and  $\Omega_m = D\Lambda_m D'$ ,  $m = 2, \dots, M$ , can be presented as  $D = WQ$  where  $Q$  is orthogonal and  $q_{ij} = 0$  when  $\lambda_{mi} \neq \lambda_{mj}$  for some  $m$ . Then observe that the  $j$ th column of  $WQ$  is a linear combination of the columns of  $W$ , with the multiplier of the  $i$ th column given by  $q_{ij}$ . Denoting  $d_0 \equiv d - d_1$ , it follows that if  $\lambda_{mi} = \lambda_{mj}$  for  $i \neq j > d_0$  and all  $m$ , but for all  $l \notin \{i, j\}$ ,  $\lambda_{ml} \neq \lambda_{mj}$  for some  $m$ , the  $j$ th column of  $WQ$  is a linear combination of the  $i$ th and  $j$ th columns of  $W$ . But if the  $j$ th column (of  $W$  and  $WQ$ ) obeys a zero constraint where the  $i$ th column obeys a strict sign constraint (condition (4)),

the multiplier  $q_{ij}$  must be zero. That is, under the conditions of Proposition 3, with  $j = d_0 + 1$  and  $i < j$ , we have  $q_{l,d_0+1} = 0$  for all  $l \neq d_0 + 1$  and  $q_{lk} = 0$  for all  $l, k = d_0 + 2, \dots, d$  such that  $l \neq k$ .

By the above discussion, when  $d_1 > 1$ ,  $Q$  is a block-diagonal matrix with two blocks in the diagonal: the first one being a  $(d_0 + 1 \times d_0 + 1)$  matrix

$$\tilde{Q} \equiv \begin{bmatrix} q_{1,1} & \cdots & q_{1,d_0} & 0 \\ \vdots & \ddots & \vdots & \vdots \\ q_{d_0,1} & \cdots & q_{d_0,d_0} & 0 \\ q_{d_0+1,1} & \cdots & q_{d_0+1,d_0} & q_{d_0+1,d_0+1} \end{bmatrix} \quad (\text{A.1})$$

and the second one a  $(d_1 - 1 \times d_1 - 1)$  diagonal matrix with  $q_{d_0+2,d_0+2}, \dots, q_{d,d}$  in the diagonal. When  $d_1 = 1$ , we simply have  $Q = \tilde{Q}$  where  $\tilde{Q}$  is as in (A.1). Consequently, for  $k > d_0$  the  $k$ th column of  $WQ$  equals to the  $k$ th column of  $W$  multiplied by  $q_{k,k}$ . It then remains to show that  $q_{k,k} = \pm 1$  for all  $k = d_0 + 1, \dots, d$ , after which one may conclude global uniqueness of the last  $d_1$  columns of the B-matrix (3.5) with arguments similar to the proof of Proposition 2.

For  $k > d_0 + 1$  (if  $d_0 > 1$ ), reasoning similar to the proof of Proposition 1 shows that  $q_{k,k} = \pm 1$ . Consider next the case  $k = d_0 + 1$  and observe that by definition the eigenvalues of  $\tilde{Q}$ , denoted as  $\gamma$ , satisfy  $\det(\tilde{Q} - \gamma I_{d_0+1}) = 0$ . Applying Laplace's expansion theorem to expand  $\det(\tilde{Q} - \gamma I_{d_0+1})$  along the last column then gives

$$(q_{d_0+1,d_0+1} - \gamma) \det \begin{bmatrix} q_{1,1} - \gamma & \cdots & q_{1,d_0} \\ \vdots & \ddots & \vdots \\ q_{d_0,1} & \cdots & q_{d_0,d_0} - \gamma \end{bmatrix} = 0 \quad (\text{A.2})$$

which implies that  $q_{d_0+1,d_0+1} = \gamma$ . Moreover,  $\tilde{Q}$  is orthogonal as the blocks in the diagonal of a block-diagonal orthogonal matrix are also orthogonal. Because  $Q$  is real and hence  $q_{d_0+1,d_0+1} \in \mathbb{R}$ , it follows that  $q_{d_0+1,d_0+1} = \pm 1$  since real eigenvalues of an orthogonal matrix are  $\pm 1$ . ■

## Appendix B Monte Carlo algorithm

We present a Monte Carlo algorithm that produces point estimates and with random initial value  $\mathbf{y}_{t-1} = (y_{t-1}, \dots, y_{t-p})$  confidence intervals for the generalized impulse response function defined in (4.1). Our algorithm is adapted from Koop et al. (1996, pp. 135-136) and Kilian and Lütkepohl (2017, pp. 601-602). We assume that the history  $\mathbf{y}_{t-1}$  follows a known distribution  $G$  which may be such that it produces a single outcome with probability one (corresponding to a fixed  $\mathbf{y}_{t-1}$ ), or it can be the stationary distribution of the process or of a specific regime. In the following,  $y_{t+n}^{(i)}(\delta_j, \mathbf{y}_{t-1})$  denotes a realization of the process at time  $t + n$  conditional on the structural shock of magnitude  $\delta_j$  in the  $j$ th element of  $e_t$  hitting the system at time  $t$  and on the  $p$  observations  $\mathbf{y}_{t-1} = (y_{t-1}, \dots, y_{t-p})$  preceding the time  $t$ , whereas  $y_{t+n}^{(i)}(\mathbf{y}_{t-1})$  denotes an alternative realization conditional on the history  $\mathbf{y}_{t-1}$  only.

The algorithm proceeds with the following steps.

0. Decide the horizon  $N$ , the numbers of repetitions  $R_1$  and  $R_2$ , and the magnitude  $\delta_j$  for the  $j$ th structural shock that is of interest.
  1. Draw an initial value  $\mathbf{y}_{t-1}$  from  $G$ .
  2. Draw  $N + 1$  realizations of a shock  $\varepsilon_t$  from  $N(0, I_d)$ . Also, draw an initial regime  $m \in \{1, \dots, M\}$  according to the probabilities pointed by the mixing weights  $\alpha_{1,t}, \dots, \alpha_{M,t}$  and compute the reduced form shock  $u_t = W\Lambda_m^{1/2}\varepsilon_t$ , where  $\Lambda_1 = I_d$ . Then, compute the structural shock  $e_t = B_t^{-1}u_t$  and impose the magnitude  $\delta_j$  on its  $j$ th element to obtain  $e_t^*$ . Finally, calculate the modified reduced form shock  $u_t^* = B_t e_t^*$ .<sup>15</sup>
  3. Use the modified reduced form shock  $u_t^*$  and the rest  $N$  standard normal shocks  $\varepsilon_t$  obtained from step 2 to compute realizations  $y_{t+n}^{(i)}(\delta_j, \mathbf{y}_{t-1})$  for  $n = 0, 1, \dots, N$ , iterating forward so that in each iteration the regime  $m$  that generates the observation is first drawn according to the probabilities pointed by the mixing weights. At  $n = 0$ , the initial regime and the modified reduced form shock  $u_t^*$  calculated from the structural shock in step 2 is used, and from  $n = 1$  onwards the  $n + 1$ th shock  $\varepsilon_t$  is used to calculate the reduced form shock  $u_{t+n} = W\Lambda_m^{1/2}\varepsilon_{t+n}$ , where  $\Lambda_1 = I_d$  and  $m$  is the selected regime.
  4. Use the reduced form shock  $u_t$  and the rest  $N$  standard normal shocks  $\varepsilon_t$  obtained from step 2 to compute realizations  $y_{t+n}^{(i)}(\mathbf{y}_{t-1})$  for  $n = 0, 1, \dots, N$ , so that the reduced form shock  $u_t$  (calculated in step 2) is used to compute the time  $n = 0$  realization. Otherwise proceed similarly to the previous step.
  5. Calculate  $y_{t+n}^{(i)}(\delta_j, \mathbf{y}_{t-1}) - y_{t+n}^{(i)}(\mathbf{y}_{t-1})$ .
  6. Repeat steps 2-5  $R_1$  times and calculate the sample mean of  $y_{t+n}^{(i)}(\delta_j, \mathbf{y}_{t-1}) - y_{t+n}^{(i)}(\mathbf{y}_{t-1})$  for  $n = 0, 1, \dots, N$  to obtain an estimate of the GIRF( $n, \delta_j, \mathbf{y}_{t-1}$ ).
  7. Repeat steps 1-6  $R_2$  times to obtain estimates of GIRF( $n, \delta_j, \mathbf{y}_{t-1}$ ) with different starting values  $\mathbf{y}_{t-1}$  generated from the distribution  $G$ . Then take the sample mean and sample quantiles over the estimates to obtain point estimate and confidence intervals for the GIRF with random initial value.

Notice that if a fixed initial value  $\mathbf{y}_{t-1}$  is of interest, step 7 is redundant.

## Appendix C Details on the empirical application

### C.1 Model selection

The maximum likelihood (ML) estimation of the models, quantile residual diagnostics, estimation of generalized impulse response functions, and other numerical analysis are carried out with the

<sup>15</sup>The independent standard normal shocks  $\varepsilon_t$  are introduced here to control random variation across the two sample paths  $y_{t+n}^{(i)}(\delta_j, \mathbf{y}_{t-1})$  and  $y_{t+n}^{(i)}(\mathbf{y}_{t-1})$ .

Model	Log-lik	BIC	HQIC	AIC	ac(2)	ac(4)	ac(6)	ac(8)
GMVAR(4, 1)	-4.092	9.816	9.189	8.768	0.681	0.000	0.000	0.000
GMVAR(1, 2)	-3.536	8.348	7.858	7.529	0.000	0.000	0.000	0.000
GMVAR(2, 2)	-3.262	8.471	7.724	7.222	0.000	0.000	0.000	0.000
GMVAR(3, 2)	-3.153	8.922	7.917	7.242	0.001	0.000	0.000	0.000
GMVAR(4, 2)	-3.057	9.400	8.138	7.290	0.203	0.448	0.264	0.010

Table 1: The log-likelihoods and values of the information criteria divided by the number of observations for the discussed GMVAR( $p, M$ ) models. The reported  $p$ -values are obtained from the quantile residuals autocorrelation test of Kalliovirta and Saikkonen (2010) employing the simulation procedure with samples of length 10000, testing for autocorrelation when taking into account 2, 4, 6 and 8 lags.

CRAN distributed R package gmvarkit (Virolainen, 2021a) that accompanies this paper. The estimation is based on the exact log-likelihood function. For evaluating the adequacy of the models, we employ quantile residual diagnostics in the framework of Kalliovirta and Saikkonen (2010) (see also the related paper by Kalliovirta, 2012, for discussion on quantile residual based model diagnostics in a univariate setting).

For a correctly specified GMVAR model, the empirical counterparts of quantile residuals are asymptotically independent with multivariate standard normal distributions and can hence be used for graphical analysis in a similar manner to the conventional Pearson residuals (Kalliovirta and Saikkonen, 2010, Lemma 3). Kalliovirta and Saikkonen (2010) also propose formal diagnostic tests for testing normality, autocorrelation, and conditional heteroskedasticity of the quantile residuals. The tests take into account the uncertainty about the true parameter value and can be calculated based on the observed data or by employing a simulation procedure for better size properties. We utilize the tests with the simulation procedure using samples of length 10000.

We started by estimating reduced form GMVAR model with  $M = 2$  regimes and autoregressive order  $p = 1$ . Then, we increased the autoregressive order until the autocorrelation test of Kalliovirta and Saikkonen (2010) passed with four lags (accounting for one year). This led to the autoregressive order  $p = 4$ , while BIC was minimized by the order  $p = 1$  and HQIC and AIC by the order  $p = 2$ . When taking into 2, 4, 6, or 8 lags, the autocorrelation tests clearly rejected the adequacy of the  $p = 1, 2, 3$  models. The  $p = 4$  model passed the tests at all the conventional levels of significance with 2, 4, and 6 lags, while it obtained the  $p$ -value 0.010 with 8 lags. As the GMVAR(4, 2) model thereby appears fairly adequate to explain the autocorrelation structure of the series, we prefer it over the inadequate lower order models that were suggested by the information criteria. The log-likelihoods and values of the information criteria (divided by the number of observations) as well as the  $p$ -values of the autocorrelation tests are presented in Table 1. We also tested conditional heteroskedasticity and normality of the quantile residuals, but since all the discussed models failed all the tests at all the conventional levels of significance, the  $p$ -values are not reported in Table 1 for brevity. More detailed discussion on the adequacy of the selected GMVAR(4, 2) model is postponed to Section C.2.

For comparison, we also estimated linear Gaussian VAR models, i.e., GMVAR( $p, 1$ ) models, with

autoregressive orders  $p = 1, \dots, 8$ . BIC was minimized by the order  $p = 1$  (9.424), HQIC by the order  $p = 3$  (9.075), and AIC by the order  $p = 4$  (8.768). The GMVAR(4, 1) model passes the autocorrelation test when taking into account 2 lags, but fails them with 4, 6, and 8 lags at all the conventional levels of significance. Our GMVAR(4, 2) model is thereby superior to its linear alternative in terms of adequacy, while it also has lower values of information criteria than any of the linear models.

It is possible that the superior fitness is due to the accommodation of time-varying covariance matrix or intercepts and cannot be attributed to the time-varying autoregression (AR) matrices. To test whether this is the case, we estimated two additional GMVAR(4, 2) models. In the first one, we constrained the AR matrices and intercept parameters to be identical in both regimes, thereby allowing for time-varying covariance matrix only. In the second one, we constrained the AR matrices to be identical in both regimes, thereby allowing for time-varying intercepts and covariance matrix only. Because the models are nested to the GMVAR(4, 2) model and the maximum likelihood estimator has the conventional asymptotic distribution under the conventional assumptions (Kalliovirta et al., 2016, Theorem 3), we can test the validity of the constraints with a likelihood ratio test. The likelihood ratio test rejects both constraints with  $p$ -values less than  $2.1 \cdot 10^{-5}$ , so it seems likely that also the AR matrices vary in time.<sup>16</sup>

## C.2 Adequacy and characteristics of the selected model

To further study the adequacy of the GMVAR(4, 2) model, we examine the quantile residual time series, sample auto- and crosscorrelation functions of the quantile residuals and squared quantile residuals, and normal quantile-to-quantile plots. The sample auto- and crosscorrelation functions (presented in Figure 3) show that there is not much auto- or crosscorrelation in the quantile residuals. The GDP deflator has an autocorrelation coefficient slightly outside the approximate bound at lag 6 and producer price index at lag 11. Also the crosscorrelation coefficient between GDP and GDP deflator is slightly outside bounds at lag 10 as well as the crosscorrelation coefficient between GDP deflator and producer price index at lag 8. Nonetheless, given that in total of 268 correlation coefficients are presented, some of them are expected to be somewhat large even when the observations are not auto- or crosscorrelated.

The squared quantile residuals have exceedingly large autocorrelation coefficients for each of the variables (presented in Figure 4), except for the interest rate, which has autocorrelation coefficients of reasonable size. There are also several large crosscorrelation coefficients, for example, between produce price index and interest rate at the lag one and between GDP and GDP deflator at the lag 16. Our model is thereby clearly inadequate to capture the conditional heteroskedasticity in the

<sup>16</sup>For robustness, we also estimated the constrained models with autoregressive orders  $p = 1, 2, 3$  (and  $M = 2$ ) and tested the validity of the constraints in these models with the likelihood ratio test. Both types of constraints were rejected for the  $p = 2, 3$  models with  $p$ -values less than 0.004, but the GMVAR(1, 2) model accepted constraining the AR matrices to be identical in both regimes with the  $p$ -value 0.222 and rejected constraining both AR matrices and intercepts with the  $p$ -value 0.006. The conclusion of likely time-varying AR matrices does not hence seem particularly sensitive to the choice of  $p$ . Notably, the validity of the likelihood ratio test requires that the unrestricted model is correctly specified, so the tests that do not use the correct autoregressive order  $p$  do not produce reliable result. If one of the orders  $M = 2$  and  $p = 2, 3, 4$  is correct, then the constraints are, nevertheless, rejected.

		<i>GDP</i>		<i>GDPDEF</i>		<i>PPI</i>		<i>RATE</i>	
	$\hat{\alpha}_m$	$\hat{\mu}_{m,1}$	$\hat{\sigma}_{m,1}^2$	$\hat{\mu}_{m,2}$	$\hat{\sigma}_{m,2}^2$	$\hat{\mu}_{m,3}$	$\hat{\sigma}_{m,3}^2$	$\hat{\mu}_{m,4}$	$\hat{\sigma}_{m,4}^2$
Regime 1	0.66	-0.54	5.04	1.20	0.43	1.25	2.91	6.39	15.73
Regime 2	0.34	0.05	1.70	0.55	0.06	0.48	2.98	3.24	8.03

Table 2: Mixing weight parameter estimates ( $\hat{\alpha}_m$ ) and marginal stationary means ( $\hat{\mu}_{m,i}$ ) and variances ( $\hat{\sigma}_{m,i}^2$ ) of the component series implied by the fitted GMVAR(4, 2) model for each of the regimes.

series.

The quantile residual time series (the top panels of Figure 5) also show some heteroskedasticity and several outliers in the quantile residuals. There is a particularly large (marginal) quantile residual of the GDP in the beginning of the Corona crisis, when the Corona lockdown caused a fast and vast drop in the cycle. Also the large drop in the commodity prices in the Financial crisis appears as a large (marginal) quantile residual.

The normal quantile-quantile-plots (the bottom panels of Figure 5) show that the marginal quantile residual distributions have excess kurtosis but are quite symmetric. The quantile residuals of GDP deflator seem slightly skewed to the right and GDP slightly to the left, however. Overall, the model's adequacy to capture the autocorrelation structure of the series seems reasonable, but conditional heteroskedasticity and (marginal) distribution are not adequately modelled.<sup>17</sup>

The estimated mixing weights of the two regimes are presented in the bottom panel of Figure 1. The first regime (blue) dominates in the late 1950's, then a period from late 1960's to mid 1980's, and finally again in the Corona crisis. The second regime (red) prevails when the first one does not: mainly in the 1960's and from the late 1980's onwards but excluding the Corona crisis. Notably, there is no regime switch in the Financial crisis.

The mixing weight parameters have the interpretation of being the unconditional probabilities for an observation being generated from each regime. For a correctly specified model, they should hence approximately reflect the proportions of observations generated from each regime. The first regime has a mixing weight parameter estimate 0.66 (shown in Table 2), and it covers approximately 33% of the series (approximated as the mean of the estimated mixing weights), whereas the second regime has the implied mixing weight parameter estimate 0.34 and it covers approximately 67% of the series.

The mixing weight parameter estimates therefore seem somewhat disproportionate to the relative number of observations from the regimes. This is possibly because the estimation puts a lot of

<sup>17</sup>The model's capability to capture the conditional heteroskedasticity and distribution of the series can be enhanced by adding a third regime. With  $p = 4$ , however, the number of parameters in each regime is rather high: 78 plus a mixing weight parameter for all but the last regime. In the most rare regime, this may be too much compared to the number of observations from that regime for any meaningful inference based on the estimates to take place. With small  $p$ , on the other hand, the model's capability to capture the autocorrelation structure of the series at larger lags might not be reasonable. Because the three regime models are also tedious to estimate in practice, we focus on the two regime models.

weight into explaining the unexpected movements caused by the Corona crisis, which requires that the probability of the second regime should start increasing already in 2020Q2 based on the previous observation in 2020Q1 (the GMVAR(4, 2) model gives the probability 0.01 for the second regime in 2020Q2, and probability 1.00 from 2020Q3 onwards). However, since the mixing weights take into account the joint likelihood of all  $p = 4$  previous observations, making the first regime probable enough based on one previous observation only requires larger mixing weight parameter. If Corona crisis is excluded from the sample and the model estimated to a series covering the period from 1954Q3 to 2019Q4, the mixing weight parameter estimates are close to the approximate number observations from each regimes (not shown). Nonetheless, as the mixing weight parameter estimates are reasonable enough not to distort the generalized impulse response functions too much, we rather include the Corona crisis and use the full available sample.

Based on the model implied marginal stationary means and variances presented in Table 2, the first regime is more recessionary than the second one, with first regime having negative and the second regime positive mean for the cyclical component of GDP. The first regime is also characterized by higher and more volatile inflation than the second regime. The mean commodity price inflation is higher in the first regime, but there is not much difference in the variances (possibly because the second regime accommodates the Financial crisis during which the commodity price inflation rate was particularly volatile). Furthermore, the stationary mean and variance of the interest rate are clearly higher in the first than the second regime. Since the first regime also prevails when the inflation rate has historically been high or volatile, we refer to it as the unstable inflation regime. Accordingly, as second regime generally exhibits lower and less volatile inflation, we refer to it as the stable inflation regime.

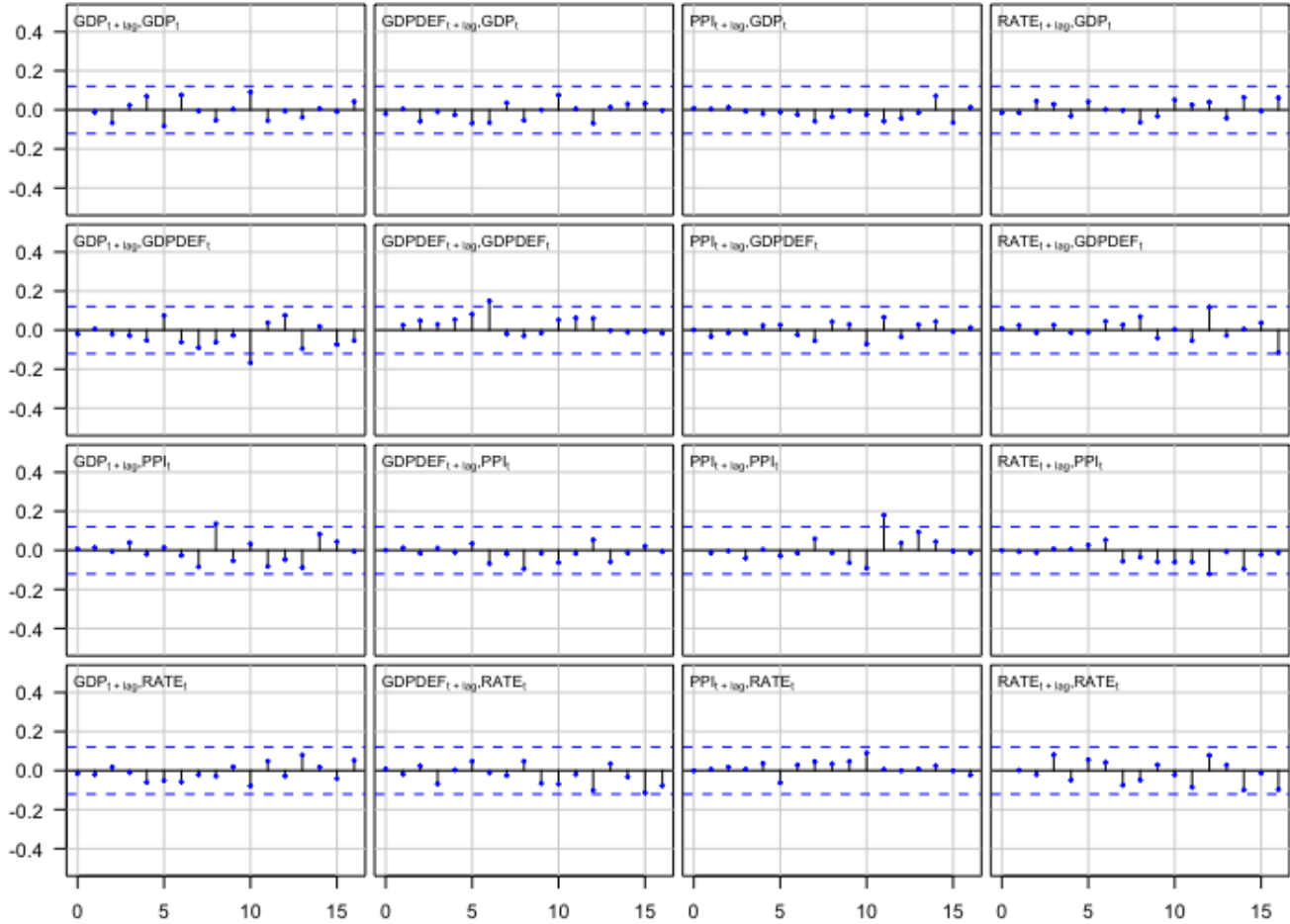


Figure 3: Auto- and crosscorrelation functions of the quantile residuals of the fitted GMVAR(4, 2) model for the lags 0, 1, ..., 16. The lag zero autocorrelation coefficients are omitted, as they are one by convention. The blue dashed lines are the 95% bounds  $\pm 1.96/\sqrt{T}$  ( $T = 263$  as the first  $p = 4$  observations were used as the initial values) for autocorrelations of IID observations, and they presented to give an approximate perception on the magnitude of the correlation coefficients.

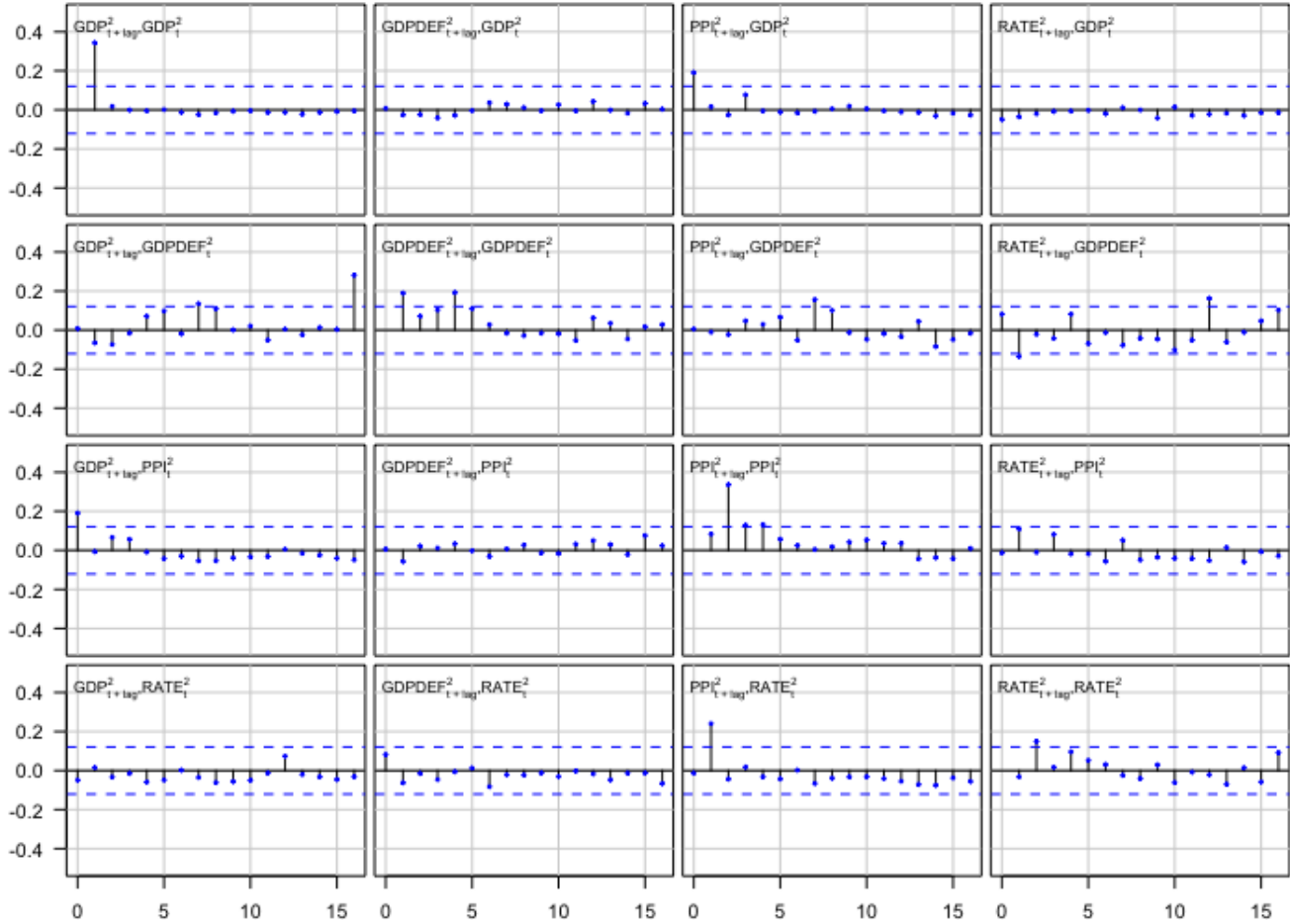


Figure 4: Auto- and crosscorrelation functions of the squared quantile residuals of the fitted GMVAR(4, 2) model for the lags 0, 1, ..., 16. The lag zero autocorrelation coefficients are omitted, as they are one by convention. The blue dashed lines are the 95% bounds  $\pm 1.96/\sqrt{T}$  ( $T = 263$  as the first  $p = 4$  observations were used as the initial values) for autocorrelations of IID observations, and they presented to give an approximate perception on the magnitude of the correlation coefficients.

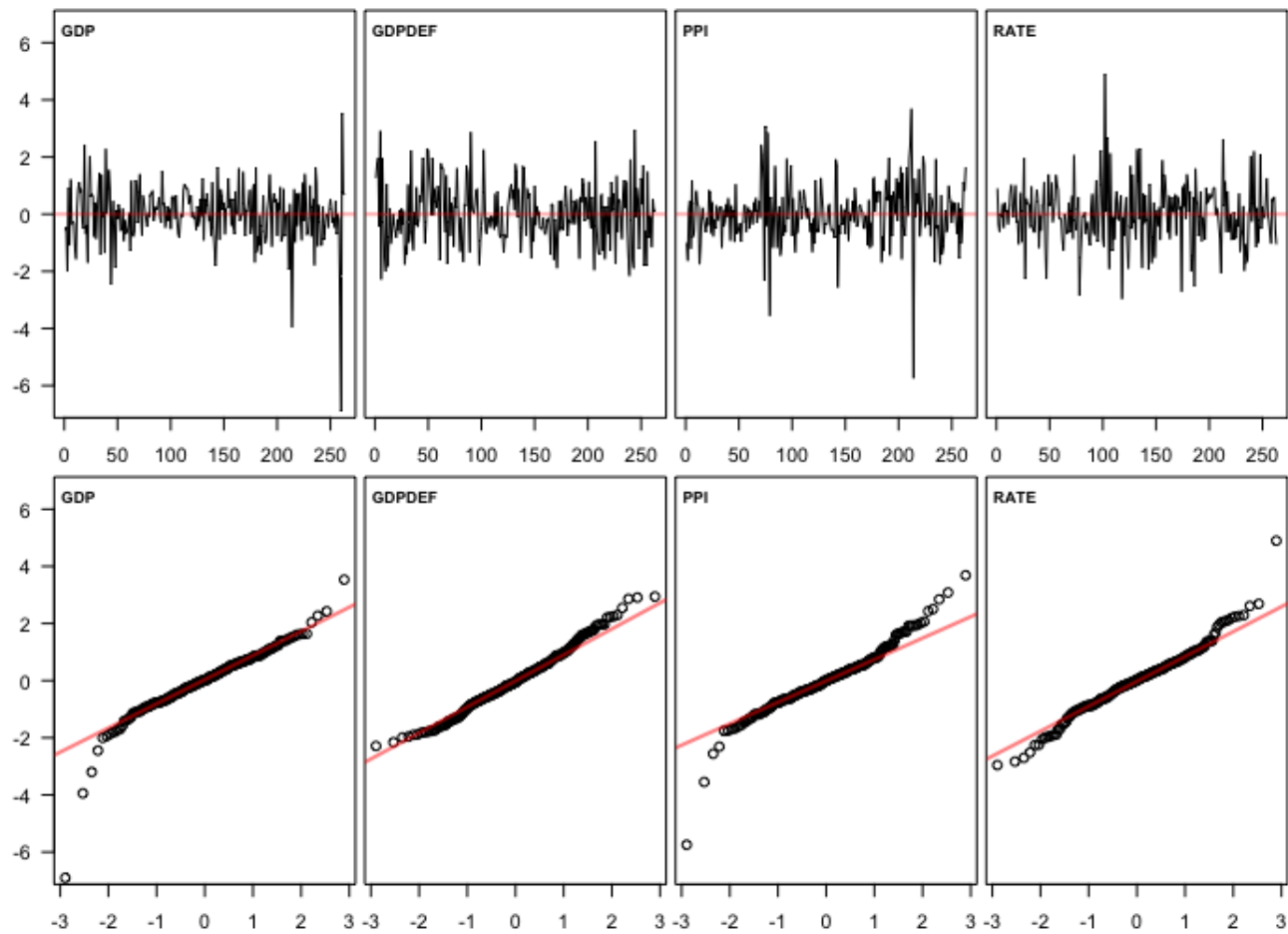


Figure 5: Quantile residual time series and normal quantile-quantile-plots of the fitted GMVAR(4, 2) model.

### C.3 Generalized impulse response functions

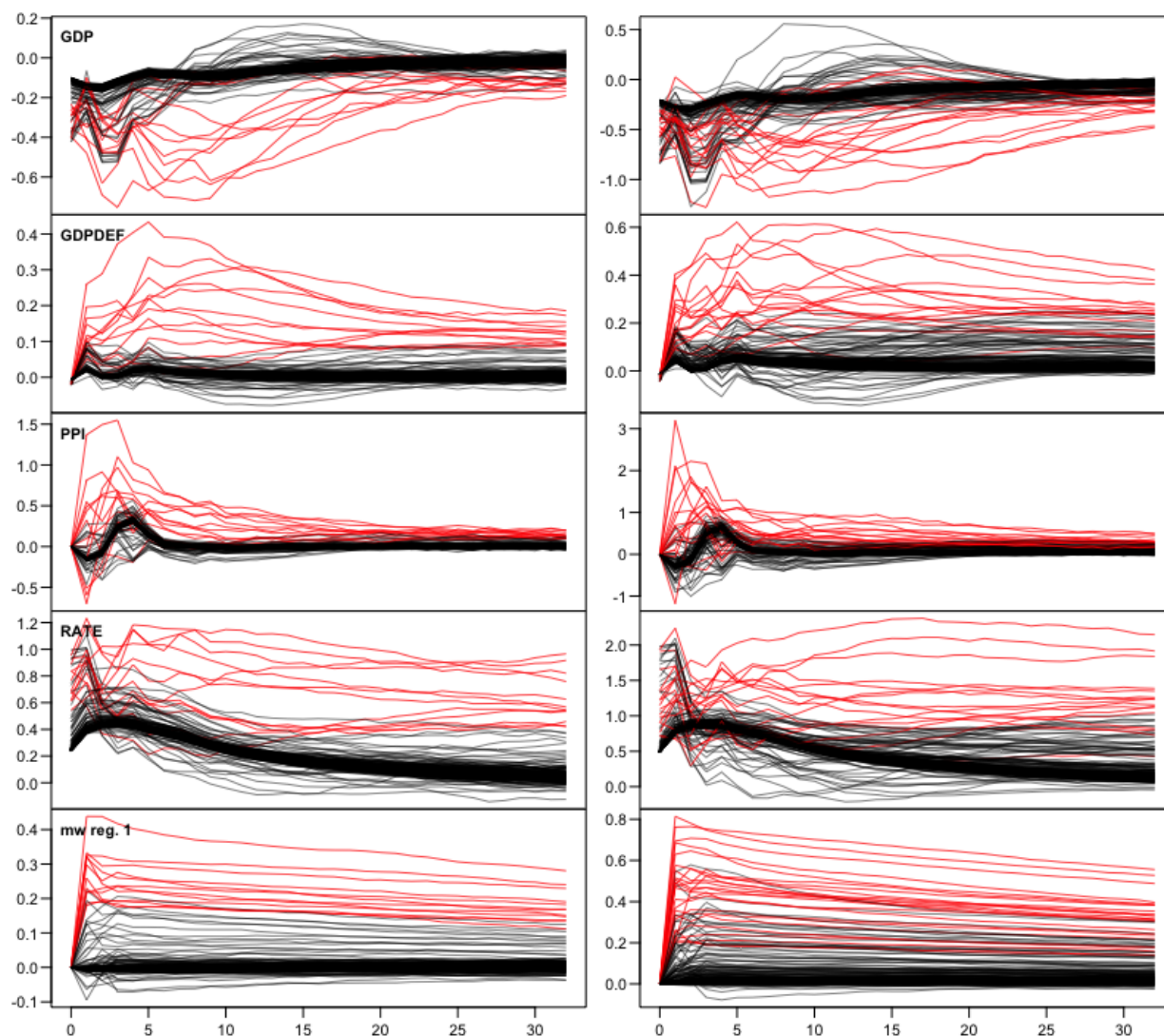


Figure 6: Generalized impulse response functions of the identified monetary policy shock of the fitted GMVAR(4, 2) model. Each panel presents 200 GIRFs, each based on random starting value drawn from the stationary distribution of the second regime and 2500 Monte Carlo repetitions. The left side panels present GIRFs to one standard error contractionary shocks and the right side panels to two standard error contractionary shocks. From the top, the first panels show the response of the cyclical component of GDP, the second panels show the response of log-differenced implicit GDP deflator, the third panels show the response of log-differenced producer price index (all commodities), the fourth panels show the response of the interest rate variable, and the bottom panels show the response of the first regime's mixing weights.

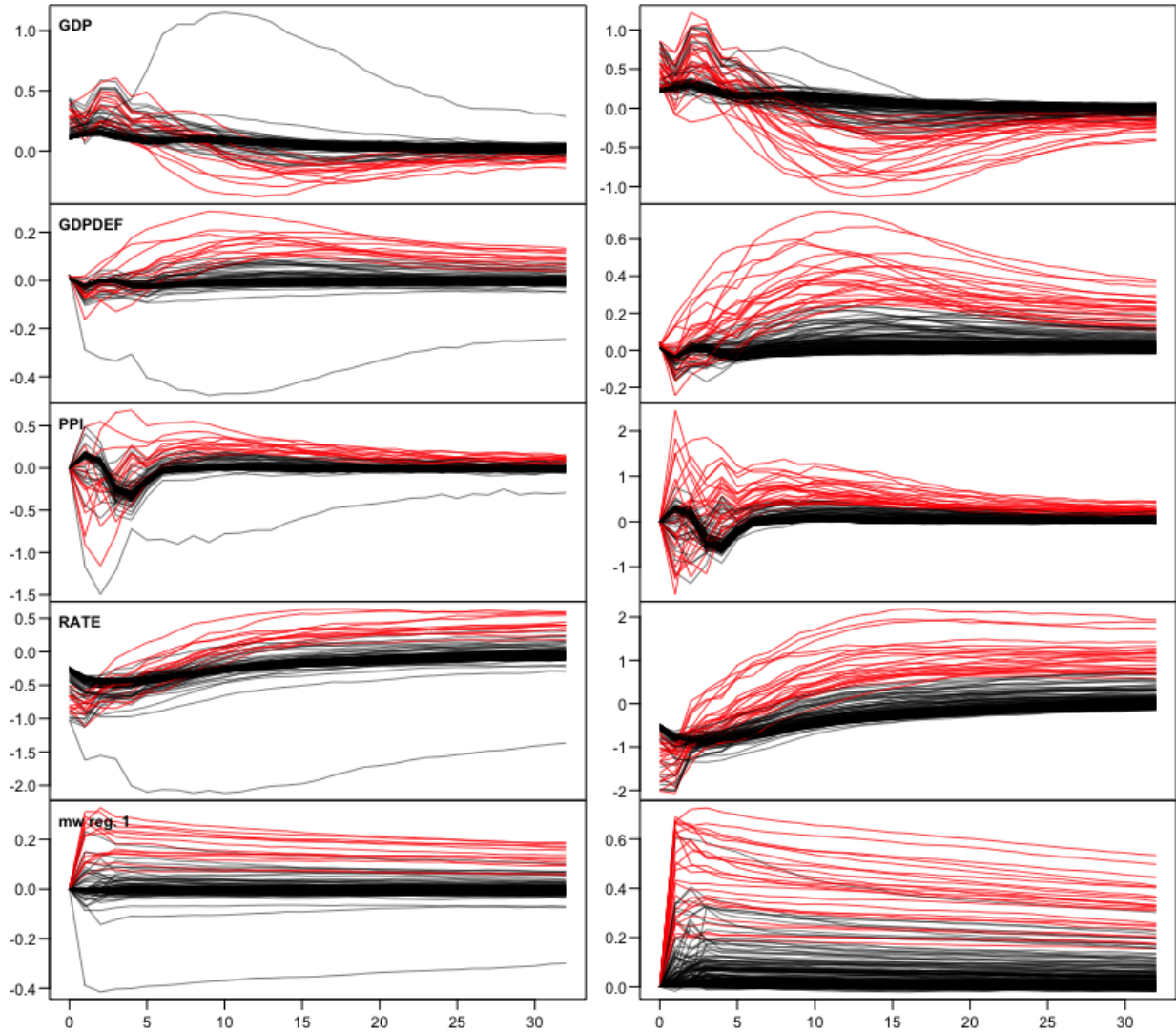


Figure 7: Generalized impulse response functions of the identified monetary policy shock of the fitted GMVAR(4, 2) model. Each panel presents 200 GIRFs, each based on random starting value drawn from the stationary distribution of the second regime and 2500 Monte Carlo repetitions. The left side panels present GIRFs to one standard error expansionary shocks and the right side panels to two standard error expansionary shocks. From the top, the first panels show the response of the cyclical component of GDP, the second panels show the response of log-differenced implicit GDP deflator, the third panels show the response of log-differenced producer price index (all commodities), the fourth panels show the response of the interest rate variable, and the bottom panels show the response of the first regime's mixing weights.